UNIVERSITÀ DEGLI STUDI DI PADOVA

Sede Amministrativa: Università degli Studi di Padova

Dipartimento di Biologia

SCUOLA DI DOTTORATO DI RICERCA IN: Bioscienze e Biotecnologie

INDIRIZZO: Neurobiologia

CICLO 27°

GABAergic interneuron communication to astrocytes: a novel modulatory signalling in brain networks

Direttore della Scuola: Ch.mo Prof. Giuseppe Zanotti

Coordinatore d'indirizzo: Ch.ma Prof.ssa Daniela Pietrobon

Supervisore: Dott. Giorgio Carmignoto

Dottoranda: Letizia Mariotti

To Federico,

who believes in me

and makes what seems impossible possible.

Abstract

Deciphering the rules governing synaptic communication among neurons is believed to provide the key to understanding how the brain works. Accumulating evidence supports, however, the novel view that the brain should not be regarded simply as a circuit of actively interacting neurons but rather as a network of neurons and astrocytes that intesively cooperate to perform computational feats. Astrocytes respond to the synaptic release of neurotransmitters with intracellular Ca^{2+} elevations mediated mainly by G-protein coupled receptors, and with the release of neuroactive molecules, collectively termed gliotransmitters, that contribute to the modulation of synaptic transmission and plasticity. The role of neuron-astrocyte interactions has been, however, intensively studied in relation to glutamatergic synaptic transmission, but little has been revealed about the role of astrocytes in GABAergic inhibitory transmission. Indeed, whether the different GABAergic interneurons specifically signal to astrocytes and what impact on the activity of local neuronal circuits this signalling pathway may are fundamental questions that have been poorly addressed. In my thesis I started to investigate the signaling between different interneurons and astrocytes, focusing on Parvalbumin (PV)- and Somatostatin (SOM)-expressing interneuron subpopulations that compose up to 70 % of the total number of GABAergic interneurons in the brain. To this aim, I developed a complex approach that combines single and two-photon laser-scanning microscopy for Ca^{2+} imaging, both in somatosensory cortex (SSCx) slices and *in vivo*, patch-clamp recording and optogenetic techniques. I found that in somatosensory and temporal cortex slices loaded with the Ca^{2+} indicator Fluo-4 AM and the astrocytic marker SR101, about 60 % of layer V astrocytes showed large amplitude somatic Ca^{2+} increases in response to GABA or baclofen (Bac, a $GABA_B$ receptor agonist) in both young and adult mice. These Ca^{2+} responses were abolished in mice lacking the inositol-1,4,5-trisphosphate (IP_3) receptor type 2 in astrocytes, while blocking $G_{i/o}$ proteins with pertussis toxin prevented Bac-mediated Ca^{2+} transients. These results reveal an involvement of the G_q/IP_3 cascade and suggest possible $G_{i/o}$-G_q protein interactions in the astrocyte response to GABA signals.

In a mouse model in which astrocytes selectively express the genetically encoded Ca^{2+} indicator $GCaMP_3$, I also found that local GABA or Bac

applications induced long-lasting Ca^{2+} oscillations at fine processes that occasionally spread to the entire astrocytic soma and other processes. I then validated the responsiveness of astrocytes to GABAergic signals in *in vivo* experiments from P30-60 anesthetized $GCaMP_3$ animals where Bac locally applied to primary SSCx layers I/II evoked Ca^{2+} elevations in 45.46 % ± 8.07 % of the total astrocytes observed.

Optogenetic stimulation of ChR_2-expressing PV or SOM interneurons also evoked astrocytes Ca^{2+} events (the average of Ca^{2+} peaks per minute significantly increase from 0.15 ± 0.06 to 0.30 ± 0.05 for PV interneurons stimulation and from 0.19 ± 0.04 to 1.16 ± 0.13 for SOM interneurons stimulation). Current pulse depolarization of a single PV or SOM interneuron increased Ca^{2+} peaks in nearby astrocytes from 0.41 ± 0.04 to 0.65 ± 0.08 ($p<0.05$) and event frequency per minute from 0.10 ± 0.31 to 1.09 ± 0.16 ($p<0.01$), respectively.

Patch-clamp recordings in the presence of TTX showed that $GABA_B$ activation triggered glutamate release in astrocytes and NMDAR-mediated slow inward currents (SICs) in nearby neurons. The frequency of SICs was strongly increased both in PV interneurons (from 0.15 ± 0.06 to 0.46 ± 0.04 event/min) and pyramidal neurons (from 0.30 ± 0.07 to 0.79 ± 0.17 event/min). The increase in SICs frequency lasted for about two minutes on average, outlasting the time of GABA agonist applications. As revealed in experiments from IP_3R2 KO mice, GABA-induced SICs were also dependent on IP_3R mediated intracellular Ca^{2+} transients in astrocytes. These data suggest that astrocytes activated by GABAergic interneurons convert a transient inhibition into a delayed excitation in local circuits.

I conclude that cortical astrocytes can be activated by two of the major GABAergic interneuron classes in the brain (PV and SOM). The consequent gliotransmitter release provides a new form of homeostatic control of local network excitability.

Riassunto

Gli astrociti hanno un ruolo centrale nella regolazione dell'attività e della plasticità dei circuiti neuronali. I processi astrocitari avvolgono le sinapsi e rispondono al rilascio neuronale di glutammato con significativi aumenti di Ca^{2+} intracellulare. Tali variazioni Ca^{2+}, principalmente mediate da recettori metabotropici, regolano il rilascio di gliotrasmettitori che modulano sia la trasmissione eccitatoria che quella inibitoria. Tuttavia, mentre l'interazione tra astrociti e neuroni eccitatori è largamente studiata, la cooperazione tra neuroni inibitori ed astrociti rimane ancora inesplorata.

L'inibizione sinaptica dipende da una varietà di interneuroni GABAergici che orchestrano l'attività spontanea e le risposte a stimoli sensoriali dei neuroni eccitatori, regolando anche lo sviluppo corticale e l'insorgenza, la propagazione e la cessazione dell'attività epilettica. L'interazione tra interneuroni ed astrociti rappresenta dunque un ulteriore livello di complessità computazionale nell'elaborazione dell'informazione nervosa ed un potenziale meccanismo alla base delle crisi epilettiche.

L'obiettivo della mia tesi è di studiare la comunicazione tra astrociti ed interneuroni, valutando se gli astrociti siano in grado di rispondere al neurotrasmettitore GABA e come la loro risposta possa eventualmente influenzare l'attività neuronale. Per caratterizzare questa interazione, ho effettuato esperimenti di imaging del Ca^{2+} in fettine corticali caricate con l'indicatore del calcio FLUO-4 AM e per marcare selettivamente gli astrociti Sulforodamina-101. Il 60 % degli astrociti monitorati ha mostrato aumenti di Ca^{2+} somatico in seguito a somministrazione di GABA o baclofen (Bac), un'agonista specifico dei recettori $GABA_B$. Tale risposta Ca^{2+} è abolita in topi KO per il recettore astrocitario dell'inositol-1,4,5-trifosfato (IP_3). D'altra parte anche il blocco delle proteine $G_{i/q}$ aboliva la risposta calcio mediata dal Bac. Questi risultati rivelano un coinvolgimento della cascata G_q/IP_3 e suggeriscono una possibile interazione tra G_i/G_q nel segnale di risposta al GABA da parte degli astrociti.

In un modello di animale transgenico in cui gli astrociti esprimono geneticamente il sensore del Ca^{2+} $GCaMP_3$, applicazioni locali di GABA o Bac hanno indotto nei processi degli astrociti oscillazioni durature e sostenute del segnale Ca^{2+}. Tale

attività Ca^{2+} occasionalmente poteva propagarsi e coinvolgere l'intero astrocita. La responsività degli astrociti al signalling GABAergico è stata inoltre validata in esperimenti *in vivo* in animali adulti P30-60 esprimenti $GCaMP_3$, dove applicazioni locali di Bac in SSCx LI/II, hanno evocato aumenti Ca^{2+} nel 45.46 % ± 8.07 % del totale degli astrociti monitorati.

Ho confermato la selettività di questa risposta in esperimenti di optogenetica, esprimendo negli interneuroni GABAergici Parvalbumina-positivi (PV) o Somatostatina-positivi (SOM) il canale foto-attivabile channelrhodopsin-2. La foto-stimolazione simultanea e selettiva dei PV o dei SOM ha dimostrato che gli astrociti rispondono al rilascio sinaptico di GABA con aumenti di Ca^{2+} mediati dal recettore $GABA_B$. Inoltre la scarica di potenziali di azione indotta in un singolo PV o in un SOM tramite una pipetta da patch recording, produce lo stesso effetto su scala locale.

Ho inoltre studiato se gli astrociti, una volta attivati da GABA, siano in grado di rilasciare glutammato evocando lente correnti depolarizzanti (SICs, slow inward currents) nei neuroni. L'imaging del Ca^{2+} accoppiato a registrazioni da neuroni piramidali hanno rivelato che l'attività Ca^{2+}, indotta dal GABA negli astrociti, provocava SICs. Infatti, esperimenti di controllo in topi IP_3R2-KO non hanno rivelato un significativo aumento nel numero di SICs. Questi dati sono stati confermati anche tramite stimolazione di PV o SOM esprimenti ChR_2 in cui, in seguito all'attivazione selettiva delle due classi di interneuroni, si è osservato un aumento significativo nella frequenza delle SICs.

Questi dati dimostrano che gli astrociti, attivati dal GABA, sono in grado di convertire un episodio inibitorio transiente, ma intenso, in un lento aumento di eccitabilità nei circuiti locali.

In conclusione, gli astrociti corticali sono attivati da due classi di interneuroni GABAergici e il conseguente rilascio di gliotrasmettitori rivela una nuova forma di controllo omeostatico dell'eccitabilità di network.

“It is the stupidest tea-party I was ever at in all my life”

Alice’s adventures in wonderland, Lewis Carroll

Contents

1. Introduction

Astrocytes are the most abundant subclass of glial cells in the brain. The term ‘glia’ is derived from the greek ‘γλια’, meaning ‘glue’. Indeed, astrocytes (together with the other glial cell types in general) have been considered for long time to function mainly as mechanical, structural and metabolic supporters of neurons. However, in the last three decades, accumulating evidence outdated this notion showing that astrocytes actively participate in the regulation of neuronal network computational processes in the neocortex. In fact, astrocytes beside exerting a broad control of brain tissue homeostasis and metabolism, contribute to brain information processing in dynamic interactions with neurons that are finely regulated in time and space. From this novel perspective the brain appear as a network of highly interactive neurons and astrocytes [6].

Most of the studies on neuron-glia interactions have focused on the excitatory principal neurons and the astrocyte response to glutamatergic transmission. As a result, our knowledge of the functional interactions between GABAergic interneurons and astrocytes is largely incomplete. Although GABAergic interneurons represent only the 20% of all cortical neurons, yet they can powerfully constrain the activity of principal neurons and shape neuronal network computations thanks to their different morphological features and diverse intrinsic membrane properties [2].

Interneuron-astrocyte reciprocal communication could represent a fundamental signalling system for the control of brain network excitability and its impairment may contribute to pathological conditions including Alzheimer’s disease, Parkinson disease, amyotrophic lateral sclerosis and epilepsy [7].

The aim of my thesis is to dissect out the relevance in the neocortex of the specific signalling between interneurons and astrocytes, addressing the following central questions: (i) Are astrocytes responsive to GABA signals? (ii) Do astrocytes respond differently to different classes of GABAergic interneurons? (iii) Do GABA-activated astrocytes signal back to either interneurons and/or principal neurons? iv) What relevance may this signalling have in local circuit excitability?

The identification and functional characterization of a reciprocal signalling between distinct GABAergic interneurons and astrocytes will open up new perspectives in our understanding not only of how the brain works but also of the cellular mechanisms at the basis of brain dysfunction.

1.1 Astrocytes

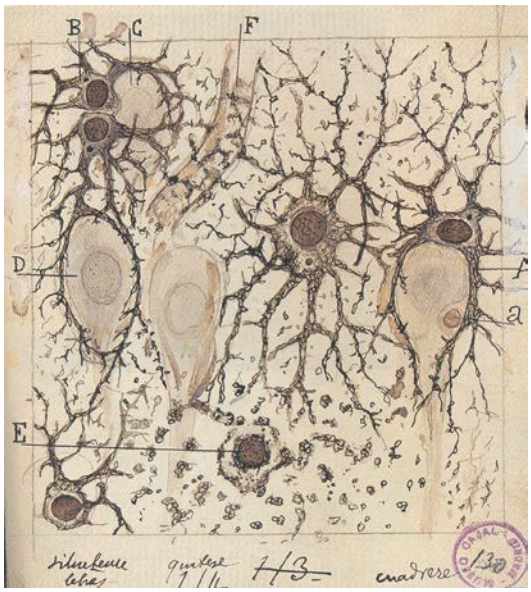

Figure 1. Cajal's drawing.
Human hyppocampal astrocytes based on brain tissue observation after Golgi method impregnation. The picture shows the fine relationship existing between neurons (C, D), astrocytes (A, B) and microvessels (F).

The first proof that the brain was populated not only by neurons but also by glial cells came from the observations made by Rudolf Virchow. In 1856 he named these structures *nevernkitt* meaning nerve-glue and later translated with the term *neuroglia*. Thirty years later, Santiago Ramon y Cajal proposed that glial cells protect neurons from incorrect electric signals and provide them with metabolic support. He also proposed a classification of glial cells with particular attention to their morphology. Indeed, he was the first to study astrocytes from a structural standpoint and, until very recently, our view of astrocytic morphology has been largely based on Cajal's metal impregnation methods. Nowadays, thanks to a number of technological advances in molecular biology, brain imaging and optogenetics, we can assert that astrocytes are characteristic star-shaped glial cells which actively participate with neurons in the computational feats performed by the brain (see below). Indeed, in a dynamic, bidirectional communication with neurons astrocytes respond with intracellular Ca^{2+} elevations to synaptic neurotransmitter release and signal back to neurons by releasing gliotransmitters which influence synaptic transmission, short and long-term plasticity and network operations.

1.1.1 Anatomy, morphology and the tripartite synapse

To understand how astrocytes functionally interact with neurons it is useful to look at their structural properties first (Fig. 1). From an anatomical point of view, astrocytes are characterized by a central soma and by a great number of processes that sense the incoming information and send signals to neighbouring cell types, as diverse as neurons, other glia and blood vessel cells. The astrocyte branches display an intricate morphological arborization composed by thick processes that ramify in dense and thinner branches as they depart from the soma. In this way, astrocytes tile the entire cortical volume, occupying non overlapping territories (100-120 μm in diameter) and enwrapping tens of thousands of synapses (Fig. 2 A, B). Each astrocyte can directly interact, in its domain, with an average of four cortical neuron cell bodies and it processes contact between 300 and 600 dendrites, the majority of which are likely to be derived from distinct parent neuronal bodies [8]. This typical domain organization helps the demarcation of functional compartments and adequate neurovascular regulation in the brain [9].

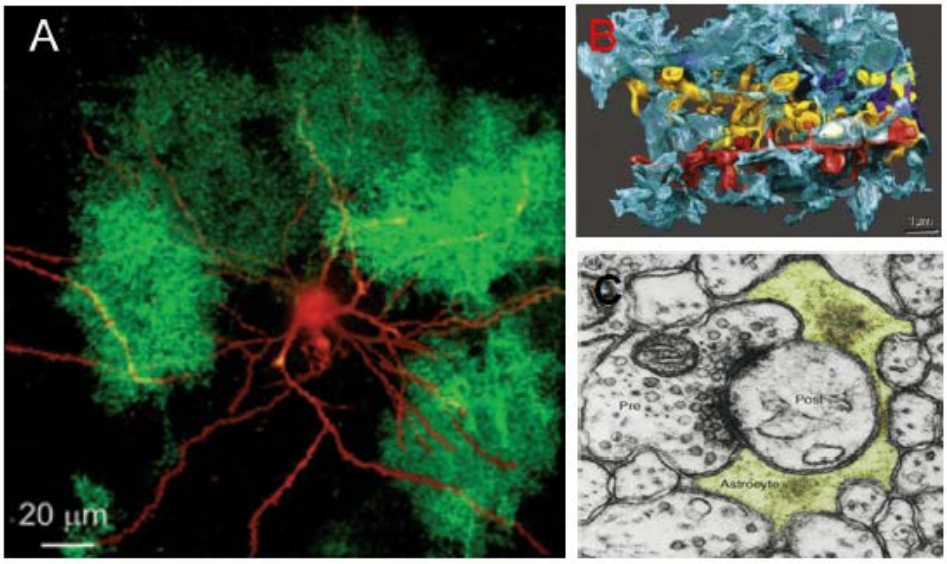

Figure 2. Astrocytes morphology. (A) Reconstruction of a biocytine-filled neuron (red) in layer II/III from a dnSNARE animal. Astrocytes (green) cover the cortical volume with non-overlapping domains. (B) 3D reconstruction of a single astrocyte process (cyan) contacting among three dendrites (yellow, red and purple). (C) Electron microscopy image of astrocyte process at the axon-spine interface revealing the presence of tripartite synapse. From [8] and [10].

Electron microscopy and immunohistochemical data reveal that each astrocyte process can contact tens of thousands of synapses (e.g. more than 50% of

hippocampal excitatory synapses are closely opposed to astrocytic processes) introducing the concept of the tripartite synapse (Fig. 2 C). In the tripartite synapse an astrocyte process enwraps the pre- and postsynaptic neuronal elements, forming a structural and functional entity that represents the information transfer unit of the brain [8].

Astrocytes processes directly contact neuronal spines and follow the movements of these plastic terminals. Hirrlinger et al. used a transgenic mice line expressing green fluorescent proteins under the GFAP promoter to image astrocytic processes adjacent to synapses in acute brain slices. They demonstrated that astrocyte processes were motile and plastic, and they can engaged and disengaged these structures [11-14]. However weather motility occurs only during development and synaptogenesis or is present in adulthood, and how this remodelling occurs *in vivo*, remain to be determined.

The astrocyte-neuron partnership has been shown to be crucial for brain physiology, not only because it modulates neuronal synaptic transmission but also because it contribute to control neurovascular coupling. Over a century ago, Golgi postulated that astrocytes represented the primary link to transfer energetic metabolites, from blood circulation to neurons (Golgi, C., 1885).

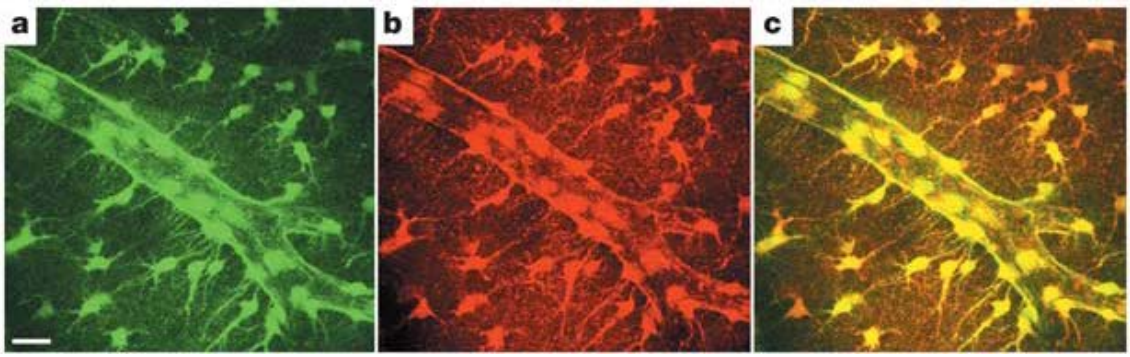

Figure 3. Two photon imaging of astrocytic endfeet (A) Two-dimensional projections showing that GFP-positive astrocytes, and the endfeet that outline an arteriole were selectively loaded with Rhod-2 (B; merged in C). From [1].

Astrocytes are indeed interposed between brain capillaries encased by specialized astrocytic processes named endfeet (Fig. 3). It is now well established that astrocytes are the fundamental elements that ensure the uptake of glucose from blood flow and, after its glycolytic processing, release

lactate which is the most abundant metabolic substrate used by neurons [15-17].

Another important property of astrocytes is their extensive intercellular coupling mediated mainly by connexin-43 and connexin-30 containing gap-junctions. Gap-junctions allow for the diffusion among many astrocytes of several ions and small molecules and the genetic ablation of these connexins profoundly impacts neuronal activity and metabolism. Glucose is taken up by astrocytic endfeet and it diffuses via gap-junctions to the multicellular astrocyte's network. This process is sensitive to AMPA receptor blockade, suggesting the involvement of post-synaptic mechanisms in recruiting astrocytic metabolic coupling [18].

For these reasons, the astrocyte appears like a hub that receives inputs from synapses and, at the same time, makes contact with the local vasculature, bridging neuronal activity and homeostasis of the extracellular environment.

1.1.2 Mechanisms of Ca^{2+} excitability

Astrocytes exhibit a form of excitability based on variations of the intracellular Ca^{2+} concentration. Unlike neurons, astrocytes are not electrically excitable cells. Therefore, they cannot integrate information in the form of electrical signals generated across the plasma membrane. Instead, astrocytes encode information as Ca^{2+} signals in the cytoplasm [10,18,5]. Astrocyte Ca^{2+} elevations can occur spontaneously, as intrinsic oscillations in the absence of neuronal activity, or in response to a neuronal input (for example: norepinephrine, glutamate, acetylcholine, histamine, adenosine and ATP have been all shown to induce Ca^{2+} elevations in glial cells in brain slice preparations [5]). They can finely tune intracellular Ca^{2+} concentrations because they express a variety of molecules involved in Ca^{2+} flows (and homeostasis), such as Ca^{2+} permeable ligand-gated channels, and an elaborate set of metabotropic receptors coupled to intracellular Ca^{2+} stores via G proteins. Activation of these signalling pathways can stimulate the phospholipase C (PLC) and the formation of inositol (1,4,5)-triphosphate ($InsP_3$), which increase the intracellular Ca^{2+} concentration through the release of Ca^{2+} from intracellular $InsP_3$-sensitive Ca^{2+} stores ($InsP_3$ receptor) [10,19]. Finally, the intracellular Ca^{2+} concentration is re-established to basal values by the activation of Ca^{2+}-ATPases positioned in the

endoplasmic reticulum (SERCAs) or in the plasma membrane. SERCAs transport the ion from the cytosol into the endoplasmic reticulum or in the extracellular space (cultured astrocytes express at least two isoforms of plasmalemmal Ca^{2+}-ATPases, i.e. isoform 1 and 4 [20]). In addition, also the Na^{+}/Ca^{2+} exchanger that have been found in cultured astrocytes (both isoforms 1 and 2), cooperates to extrude Ca^{2+} outside the cell [21].

What does the Ca^{2+} signalling mean for astrocytes? Increasing evidence suggests that the Ca^{2+} signal change induced in astrocytes by neurotransmitters, is not a stereotyped “on-off” response, but it has multiple and varied patterns and kinetics that depend on the synaptic system involved. The diversity of these signals is translated into an array of outputs, suggesting that Ca^{2+} responses in astrocytes can encode neuronal information [22,23]. Data collected until now focalized on the Ca^{2+} transients in astrocyte somata. If we take into account the Ca^{2+} signals in astrocytes cell body, we can appreciate only a part of the astrocytes ability to encode neuronal information. Somatic Ca^{2+} elevations are characterized by slow dynamics (1-10 second timescale) and occur mainly in response to an intense neuronal firing, indicating that the astrocyte soma lacks sensitivity to low levels of synaptic activity [24,25]. The new perspective to better understand astrocytes functions lies in the study of the astrocytic processes that enwrap the synaptic zone. Two recent studies demonstrated that small, rapid and localized Ca^{2+} responses can be elicited in microdomains of astrocytic processes by minimal synaptic activity (Fig. 4 A, B) [26,27]. These data suggest that astrocytes may integrate the activity of several individual synapses in processes to generate the larger Ca^{2+} responses observed in their soma upon sustained and intense neuronal activity. However, it is not clear whether the larger Ca^{2+} responses are the result of a summation of the smaller ones. Di Castro et al. (2011, [26]) reported complex spatial-temporal properties of Ca^{2+} transients in response to axonal firing in astrocytic processes, sometimes with multiple initiation points. Moreover, the rise phase of Ca^{2+} signals with slower and expanded kinetics appeared to be summative of smaller Ca^{2+} events. These observations argue against a simple propagation-dependent alteration of Ca^{2+} response.

All in all, Ca^{2+} signalling in astrocytes appears to be characterized by a complex spatial-temporal profile ranging from small, local fast responses to larger, global, albeit slower responses that result from the integration of signals derived from restricted regions of processes close to synapses. This integration appears to be governed by a nonlinear continuum of astrocyte excitability from which local changes can be incremented to larger and more global responses.

1.1.3 Chatting with neurons: gliotransmission and modulation of network activity

The Ca^{2+} elevations evoked in astrocytes by neuronal activity have important functional consequences. One of these is the release of gliotransmitters [5]. The gliotransmitters glutamate, GABA, D-serine and adenosine have been shown to act on pre- and postsynaptic elements shaping the neuronal excitability and inducing synaptic potentiation or de-potentiation. Indeed, astrocytes express protein components of exocytotic secretory machinery (SNARE complex), including the core fusion complex as well as transporters and pumps necessary for filling astrocytic vesicles with gliotransmitter [28,29]. In this way astrocytes can establish a rapid cell-to-cell communication (Fig. 5).

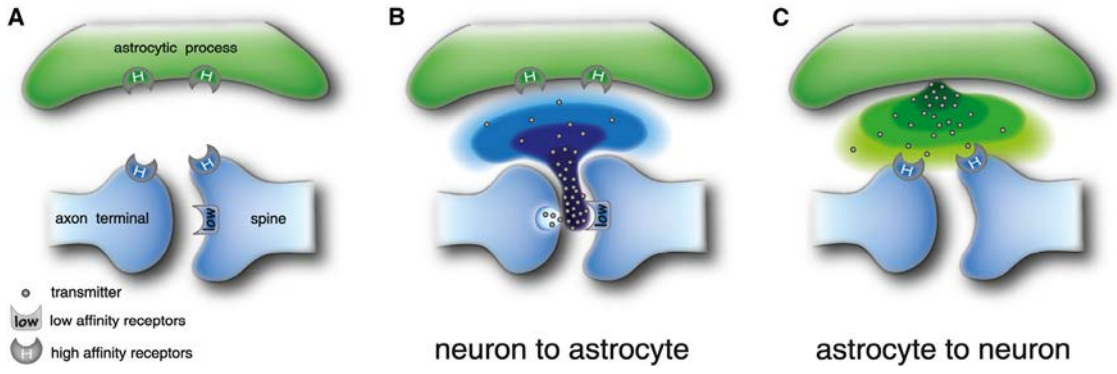

Figure 5. Bidirectional neuron-astrocyte communication. (A) Schematic drawing of the tripartite synapse illustrating the location of low- and high-affinity ligand receptors. (B) Neurotransmitter rapidly activate low-affinity receptors at the postsynaptic neuronal membrane and diffuse outside the synaptic cleft to activate high-affinity receptors at the astrocytic membrane. (C) Gliotransmitters activate high-affinity receptors at perisynaptic locations in the neuronal membrane. Decreasing neurotransmitter (B) or gliotransmitters (C) concentrations over distance from release sites is illustrated by different color intensity. From [5].

The effects of astrocyte neuromodulation depend firstly on which and where the gliotransmitter targets are located. In the CA1-CA3 hippocampal region, astrocytic glutamate has been reported to potentiate excitatory transmission by acting on postsynaptic NMDARs favouring neuronal synchrony [30,31]. On the other hand, in the hippocampal dentate gyrus the same gliotransmitter glutamate can activate presynaptic NMDARs or mGluRs to transiently potentiate excitatory transmission [32]. Moreover astrocytes, that take part of the same brain circuitry, can differently influence synaptic transmission by releasing different gliotransmitters. For example, ATP can be released in addition to glutamate and, after its conversion to adenosine, it can acts on either A_1 or A_2A receptors to depress or enhance excitatory synaptic transmission, respectively [27,33,34]. The astrocyte processes also contact numerous synapses: a stimulus received from one process, could spread through the intracellular astrocytic space in terms of Ca^{2+} wave, reaching other synapses and neurons contacted by other processes. Recently, Navarrete et al. (2008; 2010 [35,36]) found that the endocannabinoids release by neurons in CA1-CA3 hyppocampal slices activates CB_1R on astrocytes. The astrocytic CB_1R activation, in turn, determines the release of glutamate enhancing synaptic potentiation via mGluRs in relative more distant neurons. It is worth noting that endocannabinoids can also act on CB1 receptors at the presynaptic neuronal membrane and depress neurotransmitter release ([35,36]). This is an example of how astrocytes can act as a bridge in previously unknown forms of intercellular communication.

The astrocyte release of gliotransmitters is also associated to the modulation of long-term potentiation (LTP) and long-term depression (LTD) of synaptic transmission. For instance, glutamate mediates both a form of spike-timing dependent depression of excitatory transmission in the neocortex [37], but is also associated to an mGluR-dependent and NMDA-independent form of LTP in hippocampal CA1 region. This form of plasticity was demonstrated to require the coincidence between postsynaptic activity and astrocyte Ca^{2+} signalling [32]. Not only glutamate, but also D-serine is implicated in other forms of plasticity. In hippocampal CA1 region, the release of D-serine from astrocytes, which acts as NMDAR co-agonist, is necessary for the induction of NMDAR-

dependent LTP in many thousands of excitatory synapses [38]. *In vivo* experiments also demonstrate that cholinergic activity evoked by sensory stimulation induces Ca^{2+} elevations in astrocytes, determining the release of D-serine that acts on post-synaptic NMDARs, revealing another form of astrocyte-dependent LTP [39].

As discussed above, when astrocytes release glutamate they can activate neuronal NMDA receptors. Evidence for this action was provided in slice preparations from different brain regions in which glial glutamate was shown to activate NMDA receptors that contain the NR_2B subunit and to evoke slow inward currents (SICs; [30]). Measurements of SIC kinetics showed that these events are very slow compared with synaptic NMDA currents [40,30]. The mean rise time of astrocyte-evoked SICs is 60 ms, although rise times of 100–200 ms are not rare and the decay time is on the order of 400-500 ms (Fig.6).

Where are located the NMDARs that mediate the SIC? Using MK-801 to allow a use-dependent block of synaptic NMDARs, initial culture studies demonstrated that astrocytes predominantly talk to extra-synaptic NMDARs [41].

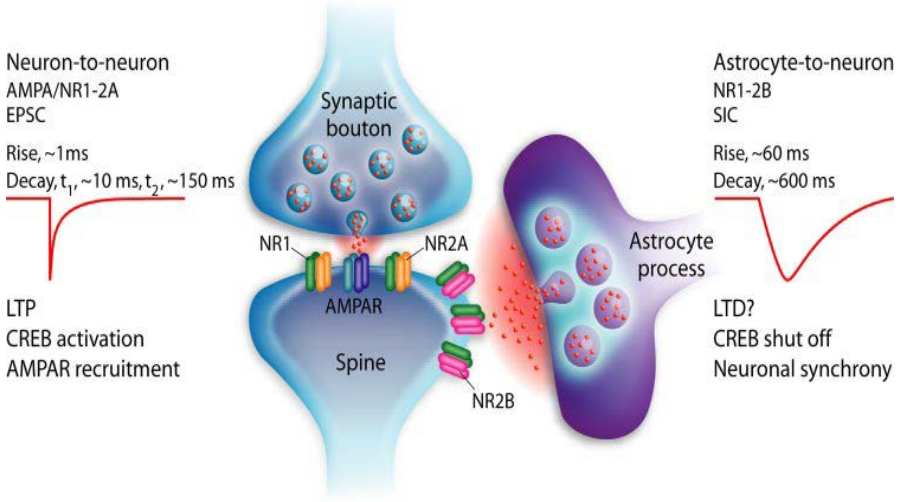

Figure 6. **Glutamate released from presynaptic terminals and from astrocytes acts on distinct NMDA receptors.** Synaptic glutamate preferentially acts on NR_2A subunit-containing NMDA receptors in addition to AMPA receptors, while astrocytic glutamate activates NR_2B subunit-containing, extrasynaptic NMDA receptors. Activation of NR_2A- and NR_2B-containing NMDA receptors leads to distinct cellular responses: synaptic NR_2A NMDA receptors lead to EPSC that means CREB activation, AMPA receptor recruitment, and LTP; while NR_2B-containing receptors have opposing actions potentially being involved in LTD, CREB shut-off, as well as promoting the synchronous activation of neurons triggering SICs. From [4].

1.2 Inhibition in the neocortex

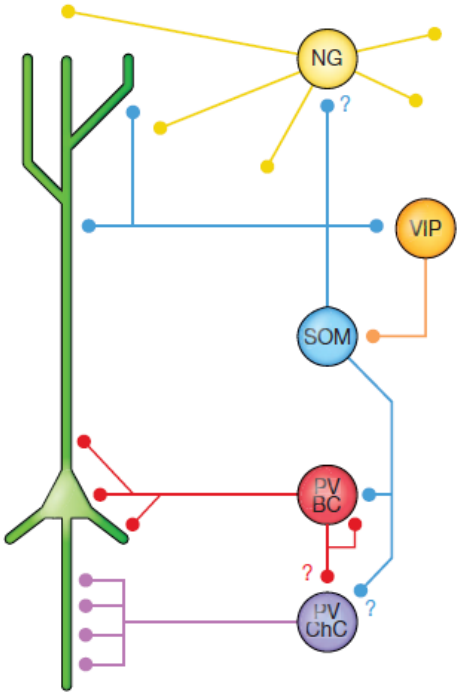

Figure 7. Schematic representation of inhibition in the neocortex. The picture shows a current understanding of the synaptic targets of five classes of cortical interneuron (PV BC, Parvalbumin Basket Cell; PV ChC, Parvalbumin Chandelier Cell; SOM, Somatostatin interneuron; VIP, Vasoactive Peptide Interneuron; NG, Neuroglial Form Interneuron), with the green neuron representing a pyramidal cell. From [3].

In the cerebral cortex, synaptic inhibition orchestrates both spontaneous and sensory-driven activity [42]. Cortical inhibition is generated by a variety of molecularly and functionally distinct types of GABAergic neurons, also referred to as interneurons (Fig. 7) ([43-46]).

An understanding of the diversity of cortical interneurons is critical to assess how the cerebral cortex can perform complex operations [44-50]. Even if they represent only a minority of all cortical neurons (10-20 % in rodents), their dense axonal arborization allow them to control the entire cortical network.

With the advent of transgenic mouse lines expressing fluorescent proteins, different subsets of interneurons could be identified and their molecular and functional properties as well as synaptic connectivity analyzed in detail. Three diverse interneuron classes that may account for nearly 100% of neocortical interneurons have been grouped according to the expression of three different markers: the Ca^{2+}-binding protein parvalbumin (PV), the neuropeptide somatostatin (SOM), and the ionotropic serotonin receptor 5HT3a (5HT3aR). Each group includes several types of interneurons that differ in morphological, electrophysiological and connectivity properties shaping differently the cortical circuit readout [51].

Morphological characteristics of GABAergic interneurons led to a precise control of the brain information flow. Indeed, each interneuron subclass differently targets specific pyramidal neurons domains in a non-overlapping manner. In this way they can modulate the cortical rhythms, playing an important role by

responding to dynamic changes in excitation, increasing the dynamic range of cortical circuits, controlling sensory receptive fields and plasticity, and maintaining the excitatory and inhibitory balance necessary for the transfer of information while preventing runaway excitation [52,45,53,54]. Moreover, interneuron dysfunctions have been implicated in a number of brain diseases ranging from epilepsy to schizophrenia, anxiety disorders and autism.

1.2.1 Parvalbumin positive interneurons

PV interneurons represent about 30% of the total number of interneurons and are capable of firing rapidly and with high temporal precision. They consist of two main subgroups: i) basket cells (including large and nest basket cells) have a typical multipolar morphology and they target preferentially soma and proximal dendrites of pyramidal neurons; and ii) chandelier cells that contact the axon initial segment of pyramidal neurons [44-46]. For their typical firing, PV interneurons are also called fast-spiking cells (FS), with little spike frequency adaptation. They show the lowest input resistance and the fastest membrane time constant of all interneurons, a feature that contributes to ensure fast synaptic responses [44,46]. Fast-spiking basket cells are likely the dominant inhibitory system in the neocortex that mediates fast, precise and powerful inhibition of target neurons. They are also involved in the feedforward inhibition which is important for creating a strict window for temporal summation of excitatory inputs and spike generation by pyramidal cells. They have been implicated also in the establishment and maintenance of fast (gamma frequency) cortical rhythms and regulation of critical-period experience-dependent plasticity.

In general, PV cells receive strong excitatory inputs from thalamus and cortex as well as inhibition from other PV interneurons [55,56]. A key role of these cells is to stabilize the activity of cortical networks: abnormalities in their behaviour can lead to different brain disorders including epilepsy and schizophrenia [57].

1.2.2 Somatostatin positive interneurons

SOM interneurons consist largely, but not exclusively, of Martinotti cells that target the tuft dendrites of pyramidal neurons as well as all the other types of

interneurons [55,56]. They are abundant in layer V, but they are present throughout layers II-VI ([51] [58]. Martinotti cells are characterized by an ovoidal soma, with bitufted dendritic morphology and an ascending axonal projection that ends with horizontal spreading brunches in layer I extended beyond a column [59,45,60]. These interneurons display a regular adapting firing pattern, but they can also exhibit an initial fire bursting behaviour with two or more spikes on slow depolarizing humps when depolarized from hyperpolarized potentials (because of this property, these cells have also been called burst spiking nonpyramidal (BSNP), intrinsic bursting (IB), or low-threshold spike (LTS) cells) [51]. Consistent with their targeting of dendritic tufts, these cells have been implicated in behaviour-dependent control of dendritic integration, as well as in more general lateral inhibition [61,62]. In contrast to PV interneurons, SOM cells receive the majority of their input from local pyramidal cells, but little inhibition or thalamic drive [55,56].

1.2.3 5HT3a receptor interneurons

5HT3aR interneurons represent about one third of the total number of GABAergic neurons in the neocortex and represent the most numerous interneurons of the cortical superficial layers. Although the classification of these neurons is still incomplete, it contains two prominent subgroups: interneurons that express the vasoactive intestinal peptide (VIP, including a group that does not express VIP) and neurogliaform cells [51].

As regards their morphology, VIP interneurons appear bitufted and multipolar. The bitufted subtype presents a vertically oriented, usually descending axon that often reaches deep layers. These neurons are characterized by irregular action potential firing discharges and for this reason they are named also irregular-spiking cells [63-67]. The multipolar subtype presents dense axonal branches that ramify extensively both in the vicinity of the cell body and toward deeper layers and, for their electrophysiological properties, are also called rapid adapting [68] or fast adapting interneurons [67]. In general, VIP neurons are characterized by the highest input resistance among the interneurons and are therefore the most excitable one. They can form synapses with shafts and spines of dendrites [44], but also with the soma of pyramidal cells. In addition,

VIP interneurons with bipolar or bitufted morphology have been shown to target mainly SOM interneurons. As a consequence, VIP interneurons have been implicated in learning and control of cortical circuits by higher-order cortex and thalamus [55,3]. Non-VIP cells represent about 60 % of 5HT3aR neurons. These cells are characterized by a small, round soma from which multiple dendrites spread radially in all directions and have a wider round axonal plexus composed of fine branches [44,51].

Finally, neurogliaform cells are thought to release GABA by volume transmission and to link multiple networks of interneurons. These cells are proposed to play a central role in generating and shaping synchronized activity of neuronal circuits. Neurogliaform cells typically have a late action potential firing [51].

1.3 GABAergic interneuron to astrocytes signalling: a neglected form of cell communication in the brain (from [2])

Given both the emerging modulatory role of astrocytes on neuronal network activities and the fast GABAergic response to local excitatory inputs, it is of interest to provide a framework that summarizes what we know about the reciprocal interactions between GABAergic interneurons and astrocytes. Currently available literature on the astrocyte response to GABAergic signals refers mainly to two different measurable effects on astrocytes of GABA applications: a membrane depolarization and an intracellular Ca^{2+} rise. Besides these functional effects, GABA significantly increases GFAP content and astrocytic branching [69], suggesting a GABA role on astrocytic maturation. In addition, a number of studies revealed that GABA inhibits proinflammatory cytokine release from astrocytes, suggesting an involvement of GABA signalling also in the modulation of inflammatory response in the brain tissue [70].

1.3.1 GABAergic interneuron signalling to astrocyes

1.3.1.1 GABA-mediated depolarization

The first evidence that astrocytes can sense GABA comes from electrophysiological experiments on cultured or acutely isolated astrocytes [71-74] and later on hippocampal, retinal and cerebellar slices [75-78]. These

studies revealed that astrocytes express functional $GABA_A$ receptors that are similar in many, though not all, aspects to those expressed by neurons. The first difference is that activation of astrocytic $GABA_A$ receptors leads to a depolarizing current in mature astrocytes, as opposed to mature neurons, due to the $Na^+/K^+/Cl^-$ cotransporter (NKCC1) expression and activity that maintains a larger amount of intracellular $[Cl^-]$ in astrocytes. The roles of GABA-mediated Cl^- efflux and astrocytic depolarization are still under investigation. It has been proposed that during intense GABAergic interneuron firing Cl^- efflux from astrocytes helps to maintain a certain $[Cl^-]_o$ level that could counteract Cl^- entry into neurons [52]. According to this view, GABA would act on astrocytes to ultimately buffer $[Cl^-]_o$ and preserve the inhibitory driving force of Cl^- ions in neurons. A recent work supports this concept and shows that gap-junction coupling is necessary to maintain astrocytic $[Cl^-]_o$ buffering capacity [79]. The authors revealed that blockage of gap junctions during intense stimulation of GABAergic transmission to CA1 neurons induced a collapse of the Cl^- gradient in these neurons. While we have to keep in mind that neurons are more sensitive to internal than external $[Cl^-]$ changes, the Cl^- efflux from astrocytes may significantly contribute to the control of $[Cl^-]_o$ at the restricted extracellular space surrounding the GABAergic synapse.

Another difference of $GABA_A$-mediated currents in astrocytes compared to those in neurons is the effect of some allosteric modulators. In particular, the benzodiazepine site inverse agonist methyl-4-ethyl-6,7-dimethoxy-beta-carboline-3-carboxylate (DMCM) acts in astrocytes, but not in neurons, as pure agonist by increasing $GABA_A$ mediated depolarizing currents [73, 80]. This result hints at a different subunit composition of the $GABA_A$ receptor complex in astrocytes with respect to neurons.

1.3.1.2 GABA-mediated Ca^{2+} responses in astrocytes

The advent of Ca^{2+} imaging techniques revealed an unexpected responsiveness of astrocytes to several neurotransmitters and molecules [55][56]. It was revealed that GABA evokes astrocytic Ca^{2+} events through different intracellular signalling pathways mediated by ionotropic $GABA_A$ receptors, metabotropic $GABA_B$ receptors as well as GABA transporters. Some

groups observed exclusively $GABA_A$-mediated responses that, by depolarizing the astrocytic membrane as reported above, activate voltage-sensitive Ca^{2+} channels (VOCCs; [74]), while other groups reported GABA-evoked Ca^{2+} events in astrocytes that were mediated exclusively by $GABA_B$ receptors [34, 81]. Furthermore, other studies in cultured astrocytes [82] and rat hippocampal slices [83], described GABA-evoked astrocytic Ca^{2+} oscillations mediated by both $GABA_A$ and $GABA_B$ receptors activation. In the latter work, the authors observed a conserved $GABA_A$-mediated response during development, while $GABA_B$-mediated response peaked during the second postnatal week and then progressively decreased. The mechanism of $GABA_B$-mediated Ca^{2+} events was shown to involve G proteins and Ca^{2+} release from internal stores [35, 83]. It is, however, unclear which G protein is responsible of the Ca^{2+} response because $GABA_B$ receptors are known to be coupled to $G_{i/o}$ proteins, at least in neurons [84], while Ca^{2+} release from internal stores usually requires G_q protein activation. Further experiments are needed to address this important aspect of astrocytic physiology. Beside the mechanism, once GABA activates Ca^{2+} oscillations in astrocytes it may, in turn, activate gliotransmission. A point of interest here is that GABA-induced Ca^{2+} oscillations in astrocytes are comparable to those induced by glutamate or others excitatory transmitters. Given that Ca^{2+} elevations represent a form of Ca^{2+}-based excitation in astrocytes, it turns out that in the neuron-astrocyte network an inhibitory GABA signal has the potential to become an excitatory signal through astrocyte activation. This leads to a number of questions: i) Do GABA and glutamate trigger a similar Ca^{2+} response in astrocytes? ii) Do individual astrocytes respond to both neurotransmitters and astrocyte subpopulations exist that respond exclusively to either GABA or glutamate? In the case an individual astrocyte can respond to both neurotransmitters, what is the ultimate effect of a simultaneous activity of the two signaling pathways? In other words, do this astrocyte integrate the signals, as it was observed in hippocampal astrocytes activated by glutamate and acetylcholine [10, 22]. Interestingly, Meier et al (2008) [83] observed that challenging astrocytes with a subthreshold stimulation with a $GABA_B$ agonist (Baclofen) increased the Ca^{2+} response to t-ACPD, i.e., an mGluR agonist. This observation suggests that a spatial and temporal

summation of different receptor-mediated Ca^{2+} signals can occur in astrocytes. For example, GABAergic and glutamatergic inputs can occur very close in time, allowing a summation of the intracellular Ca^{2+} response that may evoke gliotransmission or the modulation of important astrocytic functions.

In slices of the olfactory bulb, a region where astrocytes enwrap mainly GABAergic synapses, GABA transporters (GATs) have been shown to indirectly activate Ca^{2+} events in astrocytes from P2-7 mice [85]. In particular, Doengi et al. found that GABA-evoked astrocytic Ca^{2+} events were fully prevented by GATs blockers, but only partially by $GABA_B$ antagonists and they were not not affected by $GABA_A$ antagonists. GAT activation lead to intracellular Na^+ increase (that is co-transported with GABA) that indirectly inhibited the Na^+/Ca^{2+} exchanger. The proposed mechanism is that the consequent Ca^{2+} increase is sufficient to induce Ca^{2+} release from internal stores in a IP_3-dependent manner. The authors also showed that GABA mediates a blood vessel constriction that was blocked by GAT inhibitors, providing evidence for an important functional effect of this phenomenon.

1.3.2 GABA-activated astrocytes signal back to the neuronal network

What is the functional effect of GABA astrocyte activation on neuronal network? A main consequence of cytosolic Ca^{2+} elevations in astrocytes is the release of gliotransmitters. The frequency, amplitude, kinetics and spatial extension of the Ca^{2+} change appear to be crucial factors that determine the responsiveness of astrocytes to neuronal signals. The functional consequences of GABA signalling to astrocytes are, however, undefined and it is not conclusively proved that GABA-mediated Ca^{2+} elevations trigger the release of gliotransmitters. Furthermore, both the nature and the ultimate modulatory action on neuronal network of gliotransmitters released from astrocytes upon their activation by inhibitory signals are also unclear. Our current understanding of astrocyte-mediated modulation at inhibitory synapses is, thus, very defective, at least with respect to our knowledge of the gliotransmitter effects at excitatory synapses. Considering this important issue, we should not, however, under evaluate a few studies that provided important clues for the potential of GABA-activated astrocytes to regulate network activities. For example, in hippocampal slices,

Kang et al. [81], reported that stimulation of an intense interneuron firing induced Ca^{2+} oscillations in astrocytes and, in parallel, increased the probability of evoked unitary IPSCs. A similar increase was observed after a direct activation of individual astrocytes by mechanical stimuli or by stimulation with the selective $GABA_B$ receptor agonist Baclofen. Notably, the effect was blocked by inserting the Ca^{2+} chelator BAPTA in the astrocytic syncitium. The authors suggested that GABA activation of astrocytes leads to a release of glutamate onto the presynaptic elements that increases inhibitory synaptic transmission onto pyramidal neurons. This study provided the first evidence that synaptically released GABA activates astrocytes that, in turn modulate synaptic activity in hippocampus. A role of GABA-activated astrocytes in modulating heterosynaptic depression in the hippocampus has been revealed by Serrano et al. (2006 [34]). These authors found that tetanisation- or NMDA-induced heterosynaptic depression also evoked astrocytic Ca^{2+} oscillations and that inhibition of astrocytic Ca^{2+} responses by BAPTA abolished the heterosynaptic depression indicating that astrocyte activation was necessary for this form of synaptic plasticity. More relevant for the issue that we discuss here, the authors reported that activation of astrocytes was dependent on $GABA_B$ receptors because $GABA_B$ receptor blockade prevented both Ca^{2+} responses in astrocytes and heterosynaptic depression in neurons, while stimulation with Baclofen evoked both events. Finally, the authors found that ATP released from GABA-activated astrocytes was rapidly degraded to adenosine that inhibited glutamate release through presynaptic A1 receptor activation. The crucial role of astrocytes in mediating another form of hippocampal plasticity, i.e., the transient heterosynaptic depression, has been demonstrated by Andersson et al (2007) [86]. In this case, the authors suggested that GABA-activated astrocytes release glutamate that induces this form of synaptic depression by acting on group II/III mGluRs.

Although these studies provide compelling evidence for a contribution of GABA activated astrocytes in the modulation of synaptic activity, our knowledge of GABA-mediated gliotransmission remains unsatisfactory. It is likely that future studies will unveil multiple forms of synaptic modulations by GABA activated astrocytes (**Fig.8**).

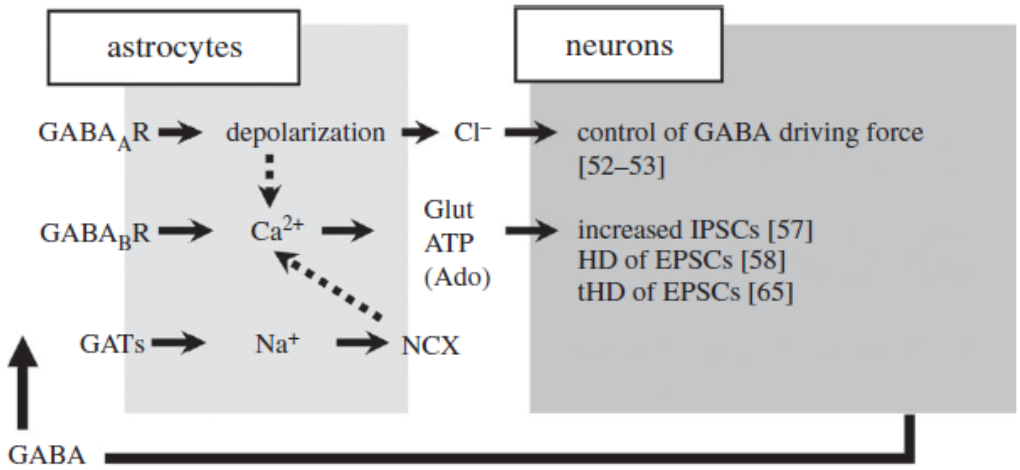

Figure 8. GABA-activated astrocytes modulate neuronal activity. Summary of the astrocytic response to GABA and the consequent signaling to neurons; dotted arrows refer to contradictory observations or limited brain regions (see §§1 and 2). Glut, glutamate; Ado, adenosine; HD, heterosynaptic depression; tHD, transient heterosynaptic depression; IPSCs, inhibitory postsynaptic currents; EPSCs, excitatory postsynaptic currents; GATs, GABA transporters; NCX, Na^+, Ca^{2+} exchanger. From [2] and for references see respectively: [71], [79], [81], [34], [86].

1.3.3 Astrocytes activated by non GABAergic signalling modulate GABAergic transmission

Astrocytes can modulate GABAergic transmission through different mechanisms. GABA transporters (GATs) expressed on astrocytic and neuronal membrane have an important functional significance in the control of the extracellular GABA concentration that sets the tone of GABAergic inhibition in local neural circuits [87-89]. In the neocortex, GAT-1 and GAT-3 are the most abundantly expressed, with GAT-1 mainly expressed in GABAergic interneurons [90] [91] and less on astrocytes, while GAT-3 is located exclusively on astrocytic processes in proximity of synapses [92]. Recent works show that astrocytic GAT-3 are important to control extracellular [GABA] also *in vivo*, particularly during periods of intense neuronal activity [93], and to shape $GABA_B$ postsynaptic currents in the thalamus [94]. Notably, in this brain region GAT-1 is selectively expressed on astrocytes [95-96], as opposed to other regions, and its role is crucial in regulating GABA tonic inhibition and thalamocortical seizures that characterize absence epilepsy [97-98].

The efficacy of inhibitory synapses in the hippocampus was recently revealed to be finely regulated by the dynamics of GAT-3 expression in astrocytes [99]. These authors found that transient receptor potential A1 channels (TRPA1) mediate frequent and localized Ca^{2+} events in astrocytes that contribute to set the resting $[Ca^{2+}]_i$. Blocking TRPA1 channels reduced resting $[Ca^{2+}]_i$ and the Ca^{2+} dependent membrane insertion of GAT-3 GABA transporters. The consequent increase in extracellular GABA concentration desensitized $GABA_A$ receptors, leading to a reduction of IPSCs on hippocampal interneurons. This work shows the importance of astrocytic TRPA1 channels in regulating the inhibitory signalling in hippocampus. It also shows the importance of resting Ca^{2+} levels for effective GABA transporters trafficking to the cell membrane.

Under certain conditions GABA transporters can reverse their function to release GABA in the extracellular space. In two separate studies Heja and colleagues (2009 and 2012) [100-101] found that astrocytes convert excitation to tonic inhibition of neurons in hippocampal slices and in *in vivo* experiments. In presence of reduced Mg^{2+} to increase network activity, they show that glutamate uptake is coupled to the reversal of GABA transporters GAT2/GAT3 that induces a GABA tonic current. The proposed mechanism is that in presence of elevated glutamatergic activity excitatory aminoacid transporters (EEATs) that co-transport with glutamate also Na^+ inside the cell (1 $glutamate^-$, $3Na^+$ and 1 H^+ inside/ 1 K^+ outside) leads to an intracellular Na^+ increase. As also GATs use Na^+ gradient to uptake GABA, this intracellular Na^+ increase may be sufficient to reverse GATs transport that start to extrude GABA. They provide evidence that this glutamate induced GABA release via EAAT/GAT transporters is also present *in vivo*. This mechanism represents a compensatory feed-back that may be protective under excessive excitatory events. Indeed the authors show that epileptic like discharges in slices are prolonged in presence of GAT blockers, suggesting that their activity during epileptic like activity is reversed and increased network inhibition [101].

Several recent works showed that astrocytes not only control $[GABA]_o$ through GABA transporters, but they can also directly affect $[GABA]_o$ by releasing GABA as a gliotransmitter. GABA in the brain is mainly synthesized in neurons by glutamic acid decarboxylases activity (GAD-65 and -67) [102]. Astrocytic GABA

content is believed to be mainly due to GATs that capture the neurotransmitter from the external space. However, several studies reported an astrocytic expression of GAD-67 and GAD-65 [70, 103-104]. For example, Lee and colleagues (2011) found in human adult tissue a GAD-65 expression in astrocytes that was comparable to that in inhibitory interneurons. In addition, GABA can be also synthesized in astrocytes starting from the polyamine putrescine [101, 105-107]. In astrocytes, GABA can be degraded by GABA-α-ketoglutaric acid aminotransferase (GABA-T) to glutamine, which is then released and subsequently captured by neurons. Most relevant to the focus of this thesis is the finding that GABA itself is released by astrocytes in many brain regions, including the olfactory bulb [108], the ventro-basal thalamus [98, 109] and the hippocampus [110]. In olfactory bulb, Kozlov and colleagues reported the first evidence that astrocytic GABA can induce slow outward currents (SOCs) in neurons. SOCs share common features with the slow inward currents (SICs) evoked by astrocytic glutamate that were observed in neurons from different brain regions [30, 111-114]. Similarly to SICs, SOCs are TTX insensitive, occur at low frequency and with significantly slower rise and decay time with respect to synaptic currents. Notably, astrocytes in olfactory bulb were able to release both GABA and glutamate to inhibit or activate synchronously groups of specific cell populations, revealing a complex astrocytic modulation of local network activity [108]. A similar dual action of astrocytes was observed in the hippocampus [110]. All in all, these results raise a number of questions on the ultimate effects of astrocytic signalling in local networks. Do glutamatergic SICs and GABAergic SOCs derive from the same activated astrocytes or do they come from different ones? As to the GABA and glutamate release, Le Meur et al. suggest that different astrocytes were likely involved because simultaneous SICs and SOCs were extremely rare. It is possible, however, that the same astrocyte may release both GABA and glutamate, but from distinct releasing sites in contact with different synapses. The mechanism of astrocytic GABA release is unclear. The fact that both in ventro-basal thalamus and hippocampal slices SOCs were increased in number upon hypo-osmotic challenge suggests a release mechanism sensitive to cell volume [109-110].

A different form of GABA release has been described in astrocytes from cerebellar slices [115-116]. In this region, GABA appears to be released by astrocytes through the bestrophin-1 (Best-1) channel, a large channel that may also allow glutamate efflux [117-118]. This astrocytic GABA release may contribute to GABA tonic inhibition of neurons that is particularly relevant in the cerebellum. As tonic inhibition can be crucial for neuronal excitability, this work opens a novel aspect in the astrocytic control of local circuit activity. Notably, GABA release has been described also in human astrocytes [119].

A recent study revealed an additional mechanism by which astrocytes regulate GABAergic inhibitory transmission. Lalo and colleagues reported that exocytosis of ATP from astrocytes modulated both phasic and tonic inhibition in somato-sensory cortex [120]. The authors showed that Ca^{2+} elevations in astrocytes evoked by TFFLR, i.e., a peptide agonist of the protease-activated receptor 1 (PAR1), lead to a vesicular ATP release that evoked P2X receptor-mediated currents in neurons. Ca^{2+} entry in neurons through P2X receptor openings lead, in turn, to a phosphorylation-dependent down regulation of $GABA_A$ receptors. In a transgenic mouse with impaired astrocytic ATP release, i.e., the dn-SNARE mouse, the IPSCs and tonic GABA currents were significantly larger. These data show that a Ca^{2+}-dependent release of ATP from astrocytes can affect the responsiveness of neurons to synaptic and extrasynaptic GABAergic signals.

Finally, astrocytes can modulate inhibition in local circuits through a direct action on GABAergic interneurons. For example, by regulating through the glutamate transporters the occupancy of the mGluRs in oriens-lacunosum moleculare interneurons, astrocytes modulate the excitability of these hippocampal interneurons [121]. A Ca^{2+} dependent release of glutamate has been also reported to activate presynaptic kainate receptors at GABAergic synapses onto inhibitory interneurons ultimately decreasing inhibitory transmission in the hippocampus [122]. An opposing effect was described for another gliotransmitter, such as ATP, that increased inhibitory synaptic transmission in the hippocampus through activation of P2Y1 receptors in interneurons [123].

Although our understanding of how GABAergic interneurons and astrocytes communicate in the neuronal network is largely undefined, these few studies hint at a richness of different mechanisms by which astrocytes can modulate GABAergic inhibition in local circuits (**Fig.9**).

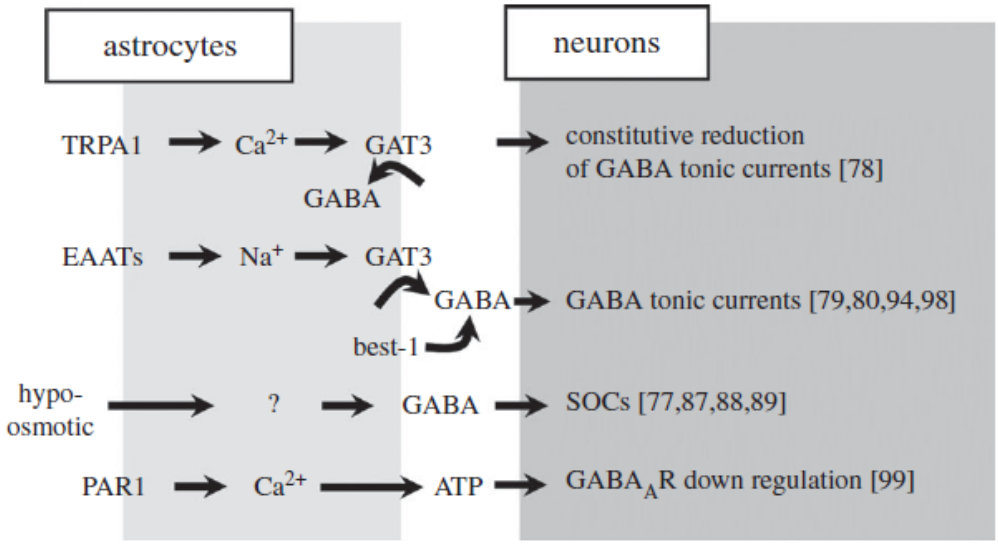

Figure 9. Astrocytes activated by different signals modulate GABAergic transmission. Summary of the astrocytic modulation of GABAergic transmission in response to different signals (see 3). TRPA1, transient receptor potential A1; GAT3, GABA transporter type 3; EAATs, excitatory amino acid transporters; Best-1, bestrophin-1; SOCs, slow outward currents; PAR1, protease-activated receptor type-1. From [2] and for references see respectively: [99], [100], [101], [115], [119], [98], [108], [109], [110], [120].

2. Open questions

A large variety of neuronal signals, including the neurotransmitter GABA, are now recognized to trigger intracellular Ca^{2+} transients in astrocytes. Astrocytes are proposed to act as space and time integrators that decode the information deriving from different neuronal signals into dynamic Ca^{2+} signal changes that either remain spatially restricted to individual or multiple processes, or recruit the entire astrocyte in a global Ca^{2+} response [5]. Based on this hypothesis, a number of questions regarding a possible reciprocal signalling between GABAergic interneurons and astrocytes needs to be answered. Firstly, does GABA released from a given class of interneurons establishes with astrocytes a specific signalling or do different classes of interneurons can similarly activate astrocytes? Secondly, do all astrocytes respond to GABA or do different

astrocyte subpopulations respond selectively to either GABA or other neurotransmitters? Thirdly, how does the GABA-mediated response integrate with other neurotransmitter-mediated responses? This is a crucial issue since glutamatergic and GABAergic signalling, as reported above, are intimately linked. Finally, has the same astrocyte the potential to release GABA as well as other gliotransmitters? Technological advances are now providing new powerful tools to address these questions and help us to fully understand the role of neuron-astrocyte communication in the brain. For example, the existence of a specific GABAergic signalling pathway between different interneuron classes and astrocytes can be investigated in mice that express the light-gated cation channel channelrhodopsin-2 selectively in a distinct class of interneurons. The use of novel genetically encoded Ca^{2+} indicators will also allow to study astrocytic Ca^{2+} responses with unprecedented time and space resolution with respect to that achieved after bulk loading with classical fluorescence Ca^{2+} indicators. This could also make possible to study neuron-astrocyte crosstalk at fine astrocytic processes located at different subcellular sites, for example at dendritic vs somatic inhibitory synapses onto principal neurons.

Given the plethora of functions played by astrocytes in brain function it is not surprising that their involvement in most neurological disorders is increasingly documented also from the very early stages of diseases, such as epilepsy, Alzheimer's Disease, Parkinson's disease, Hungtington's disease, amyotrophic lateral sclerosis, stroke and brain injury (for review see [7, 21, 124-125]). Under pathological conditions interneuron-astrocyte reciprocal interactions may also be affected. For example, it has been reported that astrocytes activated by an epileptogenic insult increase their synthetic machinery to produce neurosteroids, potent $GABA_A$ receptors modulators [126-128], that temporally prevent seizure generation and prolong the latent period in animal models of temporal lobe epilepsy [129].

In conclusion, we are only beginning to understand the dynamic interactions between distinct classes of GABAergic interneurons and astrocytes. Future studies are expected to greatly improve our knowledge in this field and have the potential to unveil novel mechanisms in brain physiology and pathology.

3. Results

3.1 Cortical astrocytes respond to GABA: from somas to processes

We first tested whether cortical astrocytes respond to GABA in slice preparations from the somatosensory cortex (SSCx) of young mice (P15-20). We loaded brain slices with the Ca^{2+} fluorescent indicator Fluo-4 AM and the selective astrocyte marker SR101 (Fig. 10 A-C) and recorded somatic fluorescence variations in astrocytes after bath perfusion with GABA receptor agonists. Experiments were performed in the presence of Tetrodotoxin (TTX, 0.5 μM) to block neuronal activity. As reported in the hippocampus [83,81,34], we found that GABA (200 μM) evoked in a significant group of cortical astrocytes a sustained Ca^{2+} response with frequent Ca^{2+} peaks (Fig. 10 C, D). Next, we performed experiments to dissect out the signalling cascade mediating GABA-induced Ca^{2+} elevations. We found that the selective $GABA_A$ receptor blocker picrotoxin (PTX, 100 μM) did not affect the GABA response (Fig. 10 C, D). Also the mean peak frequency of Ca^{2+} events increased similarly upon a GABA challenge applied in the presence of PTX (Fig. 10 C, D). Consistent with this observation, the selective $GABA_A$ receptor agonist Muscimol (Mus, 100 μM) did not change either the number of active astrocytes or the frequency of Ca^{2+} oscillations (Fig. 10 D). These data show that in the neocortex $GABA_A$ receptors are not involved in astrocytic Ca^{2+} response to GABA. Therefore, we hypothesized that astrocytes responses to GABA are mediated by $GABA_B$ receptor activation. To test this hypothesis, we perfused cortical slices with baclofen (Bac, 20-50 μM), a selective $GABA_B$ receptor agonist. We found that Bac, similarly to GABA, evoked Ca^{2+} response in a significant group of astrocytes (Fig. 10 C, D), also increasing the frequency of the Ca^{2+} transients in those astrocytes that exhibited spontaneous Ca^{2+} activity . Similar results were obtained with Bac local applications. We also found that the same astrocytes that were responsive to a first Bac local application responded to a second one with comparable Ca^{2+} increases ($\Delta F/F_0$, 171% ± 16% and 177% ± 16% upon the first and second challenge, 58 astrocytes, data not shown). Co-applications of Bac and the $GABA_B$ receptor selective antagonist SCH-50911 suppressed Bac-induced Ca^{2+} increase in astrocytes (Fig.10 C, D). Similar results were obtained in slices from auditory cortex (AuCx data not shown) where Bac

evoked similar Ca^{2+} responses in the 47.9% ± 12.1 % of active astrocytes compared to 25 % ± 9.9 % for control (94 astrocytes from 4 experiments 2 animals, p= 0.042), and the co-application of SCH-50911 prevented Bac mediated Ca^{2} elevations (22.31% ± 5.11% of a total of 60 astrocytes from 3 experiments 2 animals), indicating that GABAergic responses in astrocytes are conserved throughout the neocortex.

To further characterize how astrocytes respond to GABAergic signalling we imaged Ca^{2+} dynamics in astrocytic processes. To this aim, we used slices from $GCaMP_3$::GLAST-CreERT ($GCaMP_3$) mice, stained with SR101. These transgenic animals conditionally express the genetically encoded calcium indicator $GCaMP_3$ only in astrocytes (see methods) with good Ca^{2+} signals also at the level of thin processes that form the typical bush shaped cloud around cell body and main processes (Fig. 11 A). We analyzed the green signal variations from $GCaMP_3$ by extracting the entire process structure from the SR101 image and by subdividing it into many subregions of about 1 μm^2 (Fig. 11 B, C; see methods). We found that brief local pressure pulses of GABA (200-500 ms, 2-3 PSI) very close to a single process (15 µm on average) evoked dynamic and oscillatory Ca^{2+} signal changes across all subregions. Notably, the Ca^{2+} oscillatory behaviour persisted for one-two minutes largely outlasting the short GABA pulse duration (Fig. 11 D). We also found that astrocytes challenged with a second GABA application exhibited a larger Ca^{2+} response with respect to the first GABA application (Fig. 11 E, F), revealing a form of potentiation of the astrocyte response to GABA.

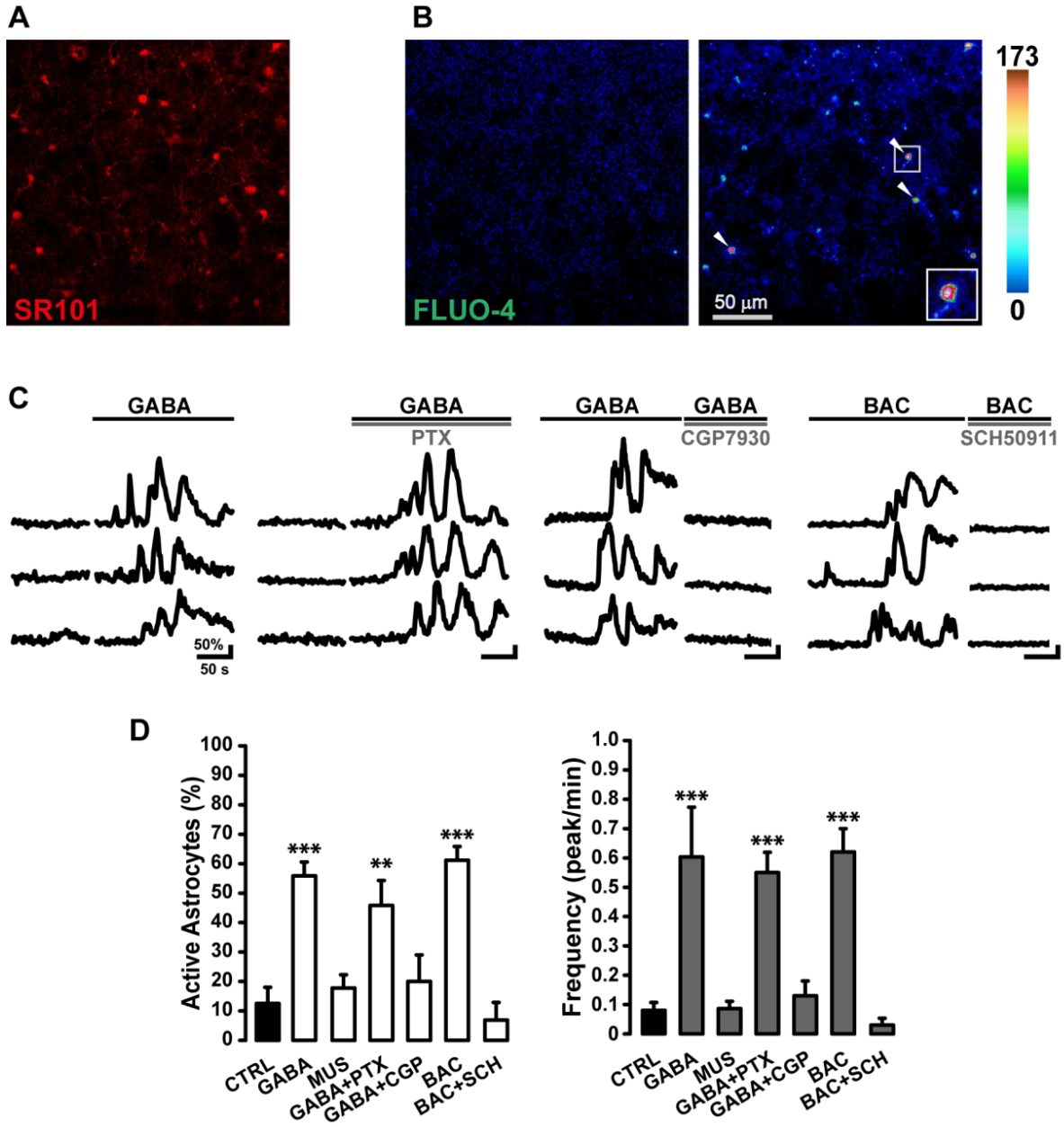

Figure10. GABA activates somatic Ca^{2+} transients in SCCx astrocytes via $GABA_BR$.

(A) Red-fluorescent SR101 selectively labels cortical astrocytes. (B) Pseudo-coloured subtractive images of FLUO-4 AM fluorescence signal acquired before (left) and after (right) GABA applications (200 µM). (C) Fluorescence signals ($\Delta F/F_0$, scale bars 50%, 50 s) over time from three astrocytes (indicated in B by arrowheads) in basal condition and after applications of different combinations of $GABA_AR$ and $GABA_BR$ agonists and antagonists. (D) Summarizing histograms showing the percentage of active astrocytes and the Ca^{2+} events frequency in different experimental conditions: GABA (GABA 200 µM; 76 astrocytes, 4 slices, 4 animals; for percentage p= 0.001727; for frequency p= 9.12 e^{-09}), muscimol (MUS, $GABA_A$ agonist 100 µM; 112 astrocytes, 5 slices, 3 animals; for percentage p= 0.6437; for frequency p= 0.8006), GABA in presence of picrotoxin (PTX 100 µM, $GABA_A$ antagonist; 125 astrocytes, 5 slices, 4 animals; for percentage p= 0.015; for frequency p= 2.547 e^{-09} frequency), GABA in presence of CGP52432 (CGP, $GABA_B$ antagonist, 117 astrocytes, 9 slices, 2 animals; for percentage p= 0.213, for frequency p= 0.11), baclofen (Bac 50 µM, $GABA_B$ agonist; 99 astrocytes, 6 slices, 3 animals; for percentage p= 3.654 e^{-05}; for frequency p= 3.4 e^{-11}), baclofen in presence of SCH50911 (SCH, $GABA_B$ antagonist 50 µM; 112 astrocytes, 4 slices, 2 animals; for percentage p= 0.761 , for frequency p= 0.588). *p<0.05, **p<0.01, *** p<0.001, p value was calculated between basal and all the other conditions.

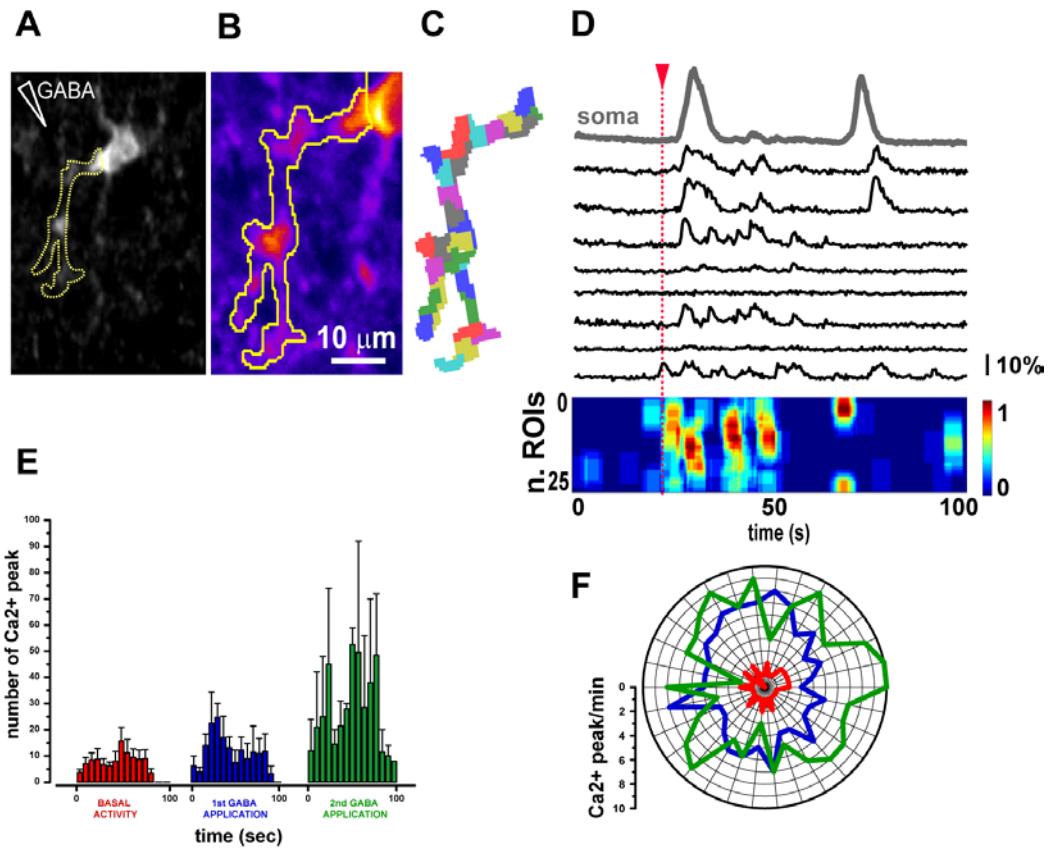

Figure 11. GABA activates long lasting Ca^{2+} transients in astrocytic processes.
(A) Two-photon Ca^{2+} imaging of an astrocyte expressing the genetically encoded Ca^{2+} indicator $GCaMP_3$.The white arrow represent the glass pipette used for GABA application. (B) Zoom of a single astrocytic process highlighted by a yellow ROI. (C, D) Segmentation in 1 μm^2 domains (left) and plot of the corresponding Ca^{2+} response time courses (right) to a brief (100 ms) local application of GABA (500 µM). The lower panel represent the cross-correlation among closest ROIs in time. Brief local pulse of GABA evokes long lasting Ca^{2+} transients involving single ROIs or the whole process. The Ca^{2+} activity lasted longer than 1 minute. (E) Peristimulus time histogram of the averaged number of Ca^{2+} peak of each subreagion divided in bin of 7 seconds (mean of 4 processes). In red the basal Ca^{2+} activity, in blue and in green the Ca^{2+} dynamics after first and the second GABA application respectively. (F) Representative radar plot for the single process reported in C. The plot shows an increase in the Ca^{2+} peaks frequency: each radius represents a subreagion and each circle a frequency value. Red area represents the baseline, while the blue and the green areas correspond to the Ca^{2+} activity after the first and the second application of GABA. (4 processes, 4 slices, 3 animals, p=0.016 for basal vs stim1, p= 2.95 e^{-05} for basal vs stim2).

3.2 $GABA_B$ receptor activation recruits Gi/o-Gq intracellular cascade in astrocytes

The cellular mechanisms at the basis of $GABA_B$ receptor-mediated Ca^{2+} transients in astrocytes are not fully clear. We first tested whether astrocytic $GABA_B$ responses involved G_i protein activation. Prolonged (4 hours) incubation of cortical slices obtained from $GCaMP_3$ mice with the G_i blocker pertussis toxin (PeTx) occluded Bac-induced Ca^{2+} events in astrocytes (Fig.12 A, B). Then, we asked whether also the IP_3 pathway is required for the observed Ca^{2+} response. To this aim, we obtained slices from inositol-1,4,5-trisphosphate (IP_3)-receptor type 2-deficient mice ($IP_3R2^{-/-}$) in which the intracellular Ca^{2+} signalling evoked by G_q-coupled receptor activation and IP_3 cascade is impaired [130], as confirmed by the absence of any Ca^{2+} responses to the mGluR agonist DHPG (Fig. 12 A, B). We found that also Bac failed to evoke Ca^{2+} elevations in any of the astrocytes studied from the TeCx and SSCx (Fig. 12 A, B). Our results demonstrate that $GABA_B$-mediated calcium responses in astrocytes involve both G_i protein activation and IP_3 intracellular cascade.

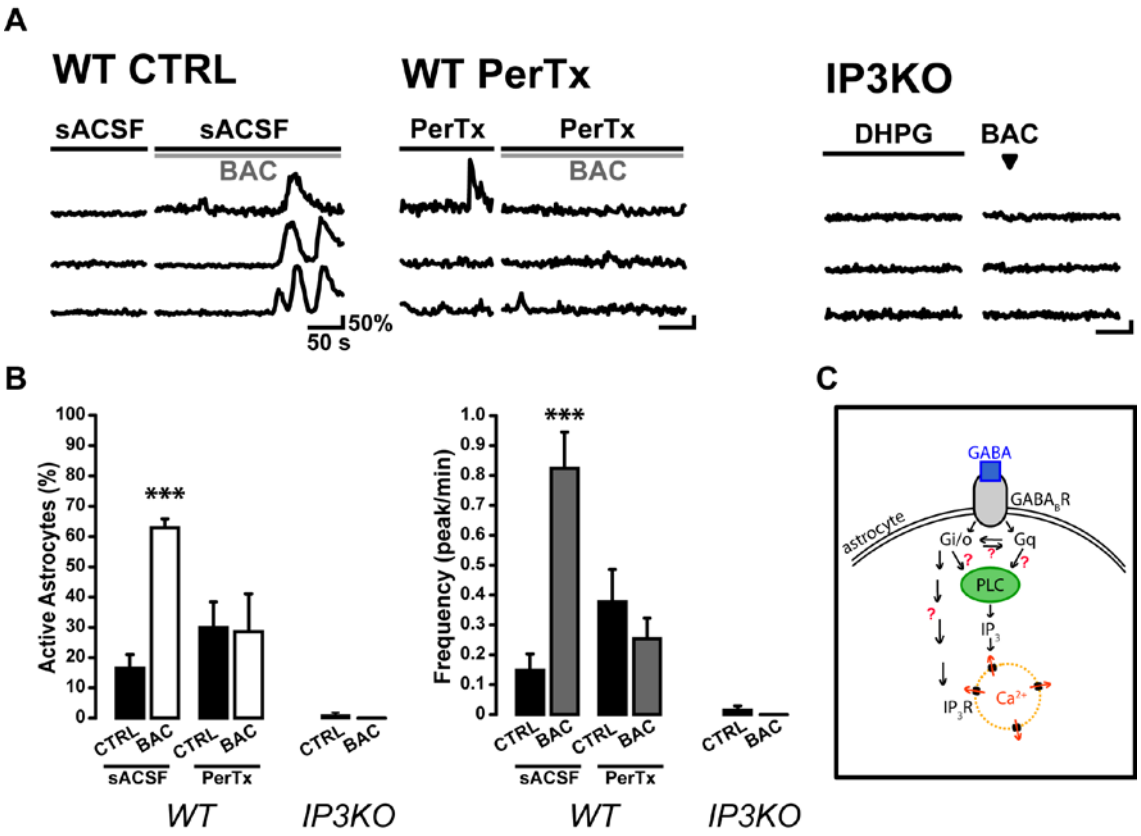

Figure 12. Astrocyte $GABA_BR$ activation recruits $G_{i/o}$ and IP_3 intracellular cascade.

(A) Astrocyte Ca^{2+} signals showing baclofen response in control (CTRL) but not after $G_{i/o}$ protein block with pertussis toxin (PerTx) nor from transgenic mice lacking astrocytic inositol-1,4,5-trisphosphate (IP_3KO). (B) Histograms showing the percentage of active astrocytes and the Ca^{2+} events per minute after baclofen applications, both in presence and absence of PerTx (53 astrocytes treated with PerTx vs 54 astrocytes in control condition, 5 experiments, 2 animals, PerTX: for percentage p= 0.93, for frequency p= 0.341; CTRL: for percentage p= 0.00012, for frequency p= 1.707 e^{-06}) and in the IP_3R2 KO mice (90 astrocytes, 7 slices, 3 animals; for percentage p= 0.337, for frequency p= 0.318). In presence of PerTx, baclofen failed to evoke astrocytic Ca^{2+} elevations (*p<0.05, **p<0.01, *** p<0.001). (C) Schematic representation of a possible $GABA_B$ receptor intracellular pathway in astrocytes.

3.3 GABA-mediated responses in astrocytes from the living intact brain from adult mice

Our results show that cortical astrocytes respond to GABA in cortical slices from young mice. We next tested whether this phenomenon is developmentally regulated by performing Ca^{2+} imaging experiments in slices from adult animals expressing $GCaMP_3$ in astrocytes (30>P>60). We found that also in these preparations Bac triggered Ca^{2+} transients in astrocytes, although the number of responsive astrocytes was reduced with respect to that in slices from young animals (Fig. 13 A, B; compare with Fig. 10). The mean peak frequency of Ca^{2+} oscillations was also significantly increased by Bac (Fig. 13 A, B). Furthermore, Mus changed neither the percentage of the active astrocytes nor the frequency of Ca^{2+} oscillations (Fig. 13 B; 48 astrocytes, 4 experiments, 2 animals). In the majority of astrocytes co-applications with GABA and SCH-50911 strongly suppressed Ca^{2+} responses to Bac (Fig. 13 A, B).

Next, we sought to validate the results obtained in brain slices in adult intact brain *in vivo*. We performed two-photon Ca^{2+} imaging in P30-60 anaesthetized animals expressing $GCaMP_3$ selectively in astrocytes. We imaged fluorescence Ca^{2+} variations in the superficial layers (LI/II) of the primary SSCx in response to local Bac applications (5 mM). We found that about half of astrocytes in the monitored area showed intracellular Ca^{2+} elevations (Fig. 13 C-F). Upon Bac applications we also measured a tenfold increase in the mean frequency of Ca^{2+} peaks (Fig. 13 E, F). To our knowledge, these data are the first demonstration that astrocyte respond to GABAergic signalling in the living brain in young adult mice.

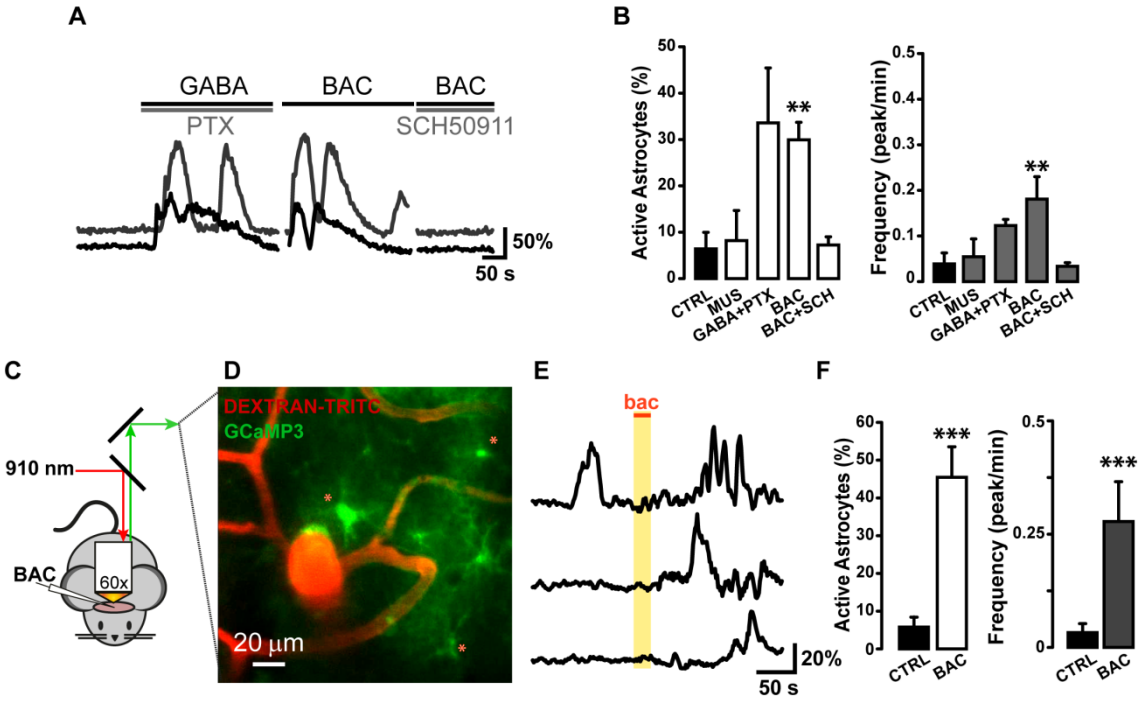

Figure 13. Local application of Baclofen triggers astrocytes Ca^{2+} transients in anaesthetized $GCaMP_3$ adult mice.

(A) Fluorescence signals ($\Delta F/F_0$) over time from two representative astrocytes acquired in basal condition and after application of different combinations of $GABA_AR$ and $GABA_BR$ agonists and antagonists. (B, E) Summarizing histograms showing the percentage of active astrocytes and the Ca^{2+} events frequency in different experimental conditions: muscimol (MUS, 100 µM; 48 astrocytes, 4 experiments, 2 animals; for percentage p= 0.915, for frequency p= 0.125), GABA (200 µM) in presence of picrotoxin (PTX, 100 µM; 45 astrocytes, 3 experiments, 3 animals; for percentage p= 0.146, for frequency p= 0.183), baclofen (BAC 50 µM; 92 astrocytes, 6 experiments, 6 animals; for percentage p= 0.004, for frequency p= 0.046 freq), SCH50911 (50 µM, 30 astrocytes, 2 experiments, 1 animal; for percentage p= 0.20, for frequency p= 1). (C) Schematic representation of *in vivo* set up. The excitation wavelength 910 nm excites both Dextran-TRITC and $GCaMP_3$ (left). Two-photon Ca^{2+} imaging of astrocytes expressing the genetically encoded Ca^{2+} indicator $GCaMP_3$. Maximal projection of blood vessels filled with Dextran-TRITC and astrocytes expressing $GCaMP_3$ in LII/III of somatosensory cortex (right). Red asterisks indicate the astrocyte soma. (D) Ca^{2+} signals from three astrocytes before and after the application of Baclofen (BAC, 5 mM). Yellow area marks the local Baclofen application. (E) Summarizing histograms showing the percentage of active astrocytes and the Ca^{2+} events frequency in control condition and after Baclofen application (4 animals; for percentage p= 0.0034, for frequency p= 2.68 $e^{-0.6}$) (*p<0.05, **p<0.01, *** p<0.001).

3.4 PV interneuron signalling to astrocytes

To evaluate whether the synaptic release of GABA from specific interneurons recruit neighbouring astrocytes, we applied optogenetic techniques to SSCx slice preparations from ChR_2-expressing PV interneurons mice after incubation with the synthetic calcium indicators Fluo-4 AM or Rhod-2 AM (depending on the ChR_2 tag). To this aim, viral vector injections were used to selectively express in cortical PV positive interneurons the light gated ChR_2 tagged either with mCherry or YFP (Fig. 14 A, B, see methods). We flashed blue LED light (473 nm; 20÷200 ms; 1÷2 Hz for 30÷60s; 1 train of 30 or 60 seconds repeated every 5 minutes; illuminated area 0.33 mm^2; mean power 38 mW/mm^2) to induce high frequency action potential firing in ChR_2-expressing PV interneurons (80÷160 Hz for Pv-ChR_2) while imaging fluorescence Ca^{2+} signals in astrocytes from LII/III or LV. Photo-stimulation of PV positive interneurons evoked Ca^{2+} elevations in astrocytes (Fig. 14 C-F). Multiple Ca^{2+} peaks were observed for approximately 100 seconds after the end of the light stimulus. After a second light stimulation of PV interneurons, the percentage of active astrocytes and the frequency of Ca^{2+} peak per minutes increased less than after the first stimulus (Fig. 14 C-F). The $GABA_B$ receptor antagonist SCH-50911 prevented the observed response demonstrating that Ca^{2+} activity in astrocytes was due to $GABA_B$ receptor activation.

We then investigated whether GABA released from a single PV interneuron can be sufficient to activate nearby astrocytes. To address this question, we used SSCx slices from tdTomato-floxed::PV-Cre mice loaded with Fluo-4 AM (Fig. 15 A). We found that an intense AP firing induced by depolarizing intracellular current pulses (200-300 pA for 100 ms at 0.5 Hz) in individual PV interneuron was followed by Ca^{2+} elevations in neighbouring astrocytes that in astrocytes already active at rest increased Ca^{2+} peak frequency (Fig. 15 A-D), while affecting the averaged amplitude of the Ca^{2+} increase. Notably, stimulation of individual PV interneurons evokes a sustained oscillatory Ca^{2+} activity in astrocytes that lasted on average for 100 seconds.

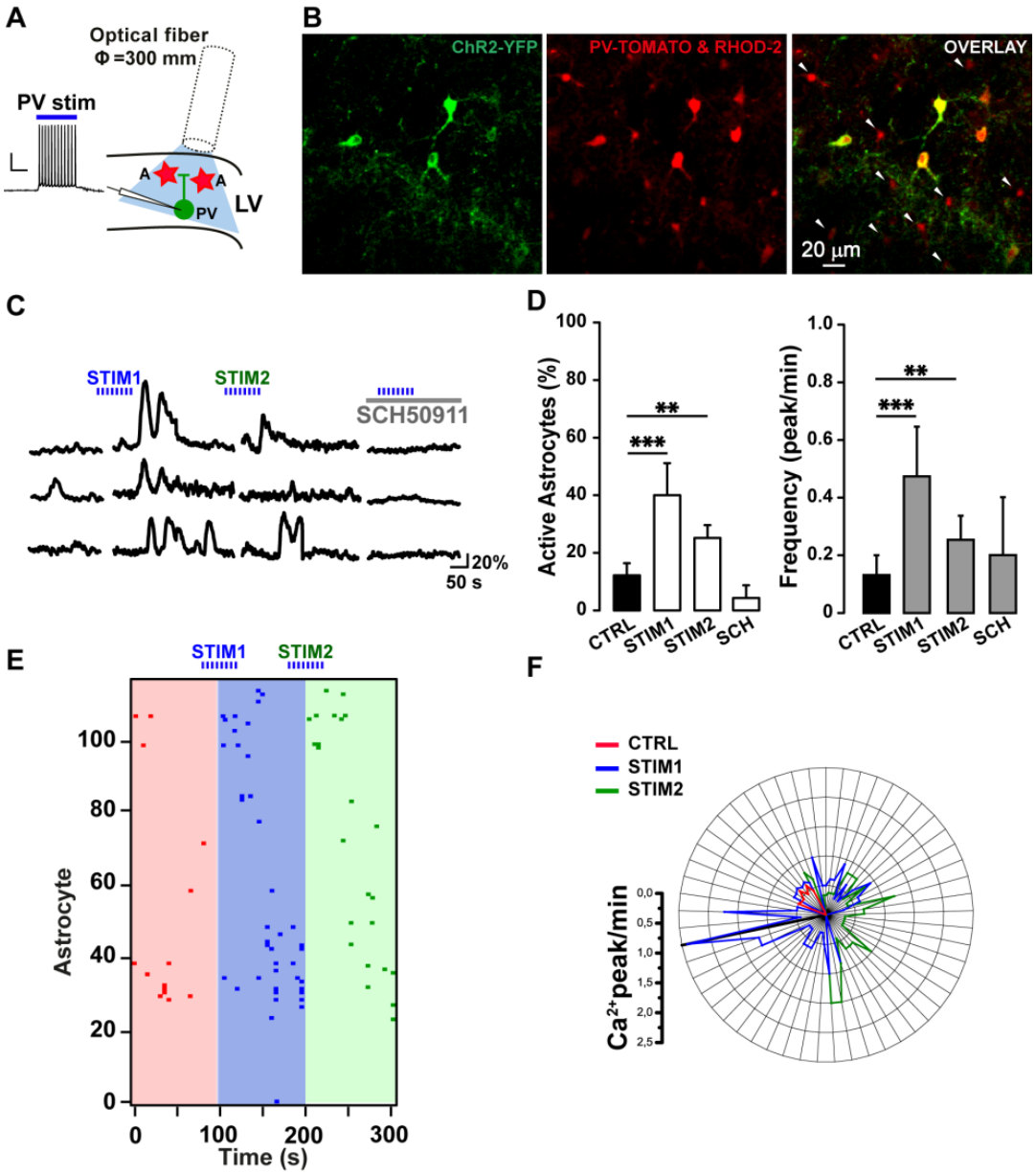

Figure 14. ChR_2 PV interneurons stimulation evokes astrocytic Ca^{2+} events.

(A) Schematic representation with the patch pipette and the optical fiber in slice of SSCx LV. Photo stimulation evoked action potentials in ChR_2-tomato expressing PV interneurons (green, scale bar 50 ms, 20 mV). Ca^{2+} imaging was performed in nearby astrocytes (LV, red stars). Blue bar represents photo stimulation (470 nm, 150 ms, 1.4 mW) (B) Confocal image of ChR_2-yfp expressing interneurons (left), PV expressing tomato and astrocytes loaded with Ca^{2+} indicator Rhod-2 (middle) and the overlay (right) where interneuron are visible in yellow, while astrocytes in red. Arrowheads mark putative astrocytes. (C) Ca^{2+} dynamics from three astrocytes before and after blue light stimulation (dashed blue line; 480 nm laser pulses, 200 ms, 1 Hz, repeated for 1 min). Perfusion with $GABA_BR$ antagonist SCH-50911 (50 µM) abolished light induced Ca^{2+} responses. (D) Summary of the average percentage of active astrocytes and Ca^{2+} peak frequency under different conditions (111 astrocytes, 8 experiments, 5 animals; for percentage: p= 0.034 (CTRL vs STIM1), p= 0.052 (CTRL vs STIM2), p= 0.23 (CTRL vs STIM2), For frequency: p= 0,00005 (CTRL vs STIM1) p= 0,00379 (CTRL vs STIM2) p= 0,27123 (CTRL vs STIM2) (*p<0.05, **p<0.01, *** p<0.001). (E) Raster plot showing the Ca^{2+} peak trend of all astrocytes over time. Each line corresponds to an astrocyte and each dot corresponds to a Ca^{2+} peak. Red area is the basal activity; blue and green areas are after the first and second PV photo-stimulation, respectively. (F) Radar plot of the astrocytes showed an increase in the Ca^{2+} peaks frequency: each radius represents an astrocyte and each circle is a frequency value. Red line represents the baseline while the Ca^{2+} activity after the first and the second light stimulation are represented by the blue and the green lines, respectively.

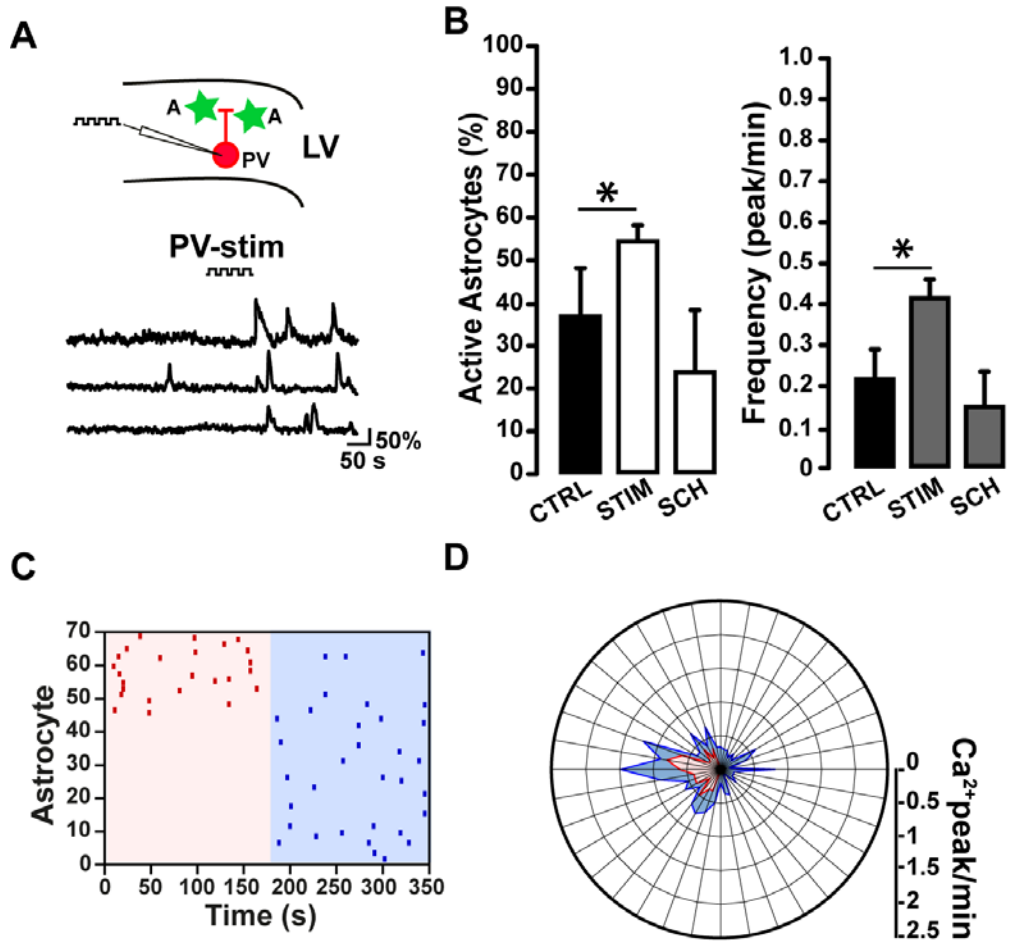

Figure 15. Stimulation of a single PV interneuron evokes astrocytic Ca^{2+} events.
(A) Schematic experimental representation (upper panel) showing the patch pipette to selectively stimulate a PV expressing interneuron in LV while performing Ca^{2+} imaging from astrocytes loaded with FLUO-4 AM in LV (green stars). In the lower panel the time course of Ca^{2+} changes in three astrocytes from SSCx LV before, during and after induction of action potential firing in a single PV cell. (B) Summarizing histograms showing the percentage of active astrocytes and the mean Ca^{2+} peak frequency before and after the stimulation of a single PV interneuron. The application of $GABA_B$ receptor antagonist almost completely abolished the astrocytes Ca^{2+} activity. (74 astrocytes, 7 experiments, 4 animals; for percentage p= 0.0042, for frequency p= 0.0025., *p<0.05, **p<0.01, *** p<0.001). (C) Raster plots of Ca^{2+} peaks over time for all astrocytes monitored. Red area represents basal Ca^{2+} activity with some astrocytes exhibiting spontaneous Ca^{2+} oscillations, while the blue area represents Ca^{2+} activity after PV single cell stimulation. (D) Radar plot of the Ca^{2+} peak frequency before (red) and after (blue) stimulation of a PV interneuron. Radii represent only astrocytes showing an increase in Ca^{2+} peak frequency and circles represent the Ca^{2+} frequency value.

3.5 SOM interneuron signalling to astrocytes: sensitivity and plastic responses

Optogenetic techniques were used to selectively stimulate SOM positive interneurons while monitoring Ca^{2+} dynamics in astrocytes from layers II/III and V. Similarly to what reported above, ChR_2 was specifically expressed in cortical SOM positive interneurons (see methods). We found that after light stimulation of ChR_2-expressing SOM interneurons (20÷200 ms; 1÷2 Hz for 30÷60s; 1 train of 30 or 60 seconds repeated every 5 minutes; evoked firing frequency, 30-150 Hz) a large group of astrocytes showed Ca^{2+} transients with an increased Ca^{2+} peak frequency (Fig. 16 A-D). Interestingly, after the second light stimulation both the percentage of active astrocytes and the Ca^{2+} peak frequency significantly increased, suggesting a form of plasticity in the astrocyte response to successive GABA stimulations (Fig. 16 C-F). The duration of evoked Ca^{2+} responses was 105 seconds, on average. $GABA_B$ receptor antagonists almost completely prevented astrocyte responses to SOM stimulation (Fig. 16 C-F).

We also evaluated the Ca^{2+} response evoked in astrocytes by the firing activity in individual SOM interneurons. In SSCx brain slices from GIN mice (see methods) we stimulated individual SOM interneurons through depolarizing current pulses as described above for the PV interneurons. We found a significant Ca^{2+} increase in about half of the monitored astrocytes upon SOM interneuron stimulation. The mean Ca^{2+} peak frequency was also significantly increased after SOM stimulation (Fig. 17 C-D). Evoked Ca^{2+} elevation were recorded in astrocytes up to 100 seconds after the stimulation.

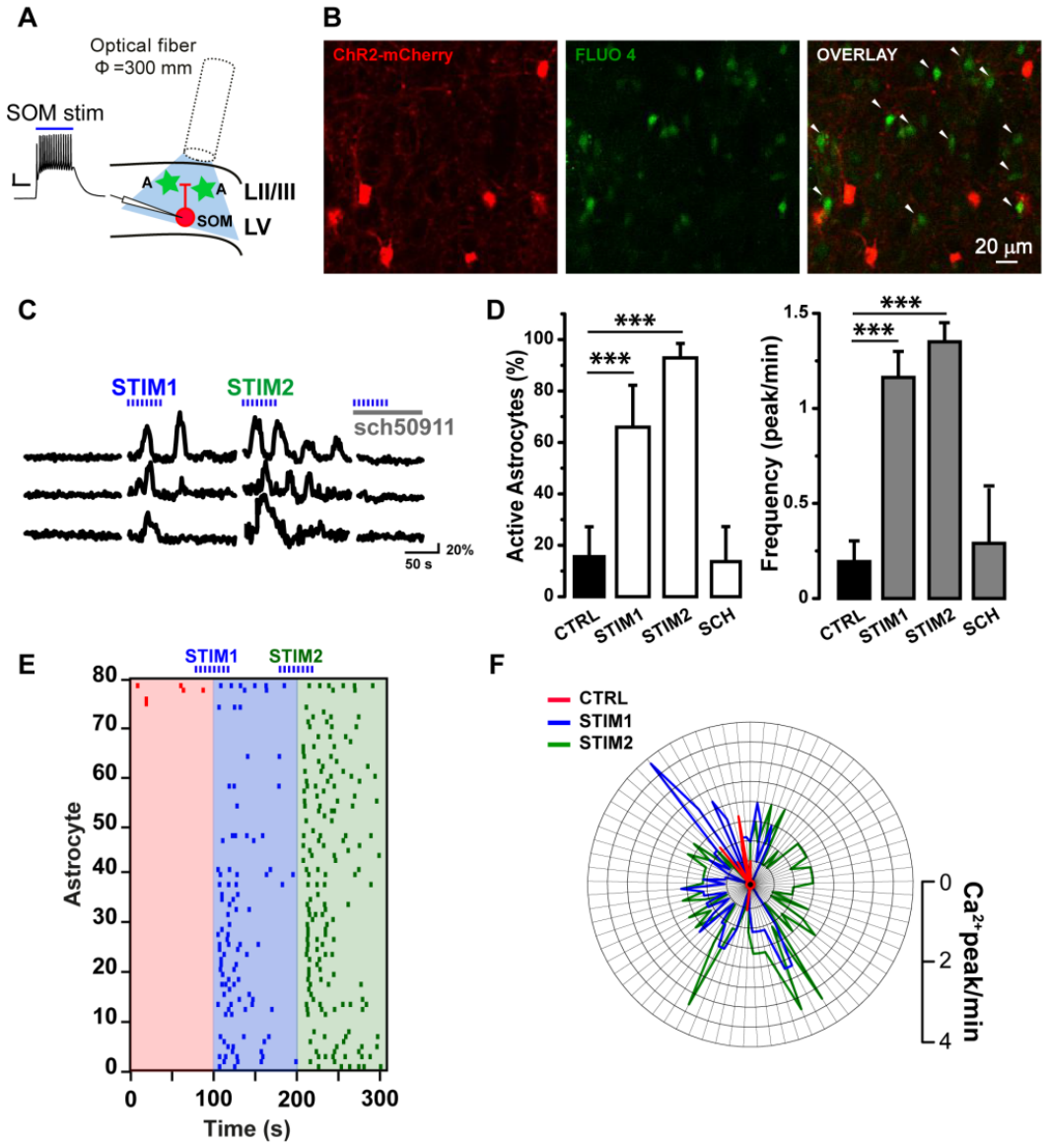

Figure 16. ChR_2 SOM interneurons stimulation triggers plastic Ca^{2+} responses in downstream astrocyte. (A) Schematic representation with the patch pipette and the optical fiber in slice of SSCx LV. Photo stimulation evoked action potentials in ChR_2-mCherry expressing SOM interneurons (red) (scale bar 10 mV, 100 ms). Ca^{2+} imaging was performed in LII/III astrocytes (green stars). Blue bar represents photo stimulation (470 nm, 150 ms, 1.4 mW). (B) Confocal image of ChR_2-mCherry expressing interneurons (left), astrocytes loaded with Ca^{2+} indicator FLUO-4 AM (middle) and the overlay (right) where interneuron are visible in red, while astrocytes in green. Arrowheads mark putative astrocytes. (C) Ca^{2+} dynamics from three astrocytes before and after blue light stimulation (dashed blue line, 480 nm laser pulses, 200 ms, 1 Hz, repeated for 1 min). Perfusion with $GABA_BR$ antagonist SCH-50911 (50 µM) abolishes light induced Ca^{2+} responses. (D) Summary of the average percentage of active astrocytes and Ca^{2+} peak frequency under different conditions (147 astrocytes, 6 experiments, 2 animals; for percentage: p= 0.04 (CTRL vs STIM1), p= 0.00013 (CTRL vs STIM2), p= 0.26 (STIM1 vs STIM2), for frequency: p= $1.12e^{-10}$ (CTRL vs STIM1) p= 1.16 e^{-22} (CTRL vs STIM2), p= 0.002 (STIM1 vs STIM2) p= 0.59 (SCH conditions), *p<0.05, **p<0.01, *** p<0.001). (E) Raster plot showing the Ca^{2+} peak trend of all astrocytes over time. Each line corresponds to an astrocyte and each dot corresponds to a Ca^{2+} peak. Red area is the basal activity; blue and green areas are after the first and second SOM photo-stimulation, respectively. (F) Radar plot of the astrocytes showed an increase in the Ca^{2+} peaks frequency: each radius represents an astrocyte and each circle is a frequency value. Red line represents the baseline while the Ca^{2+} activity after the first and the second light stimulation are represented by the blue and the green lines respectively.

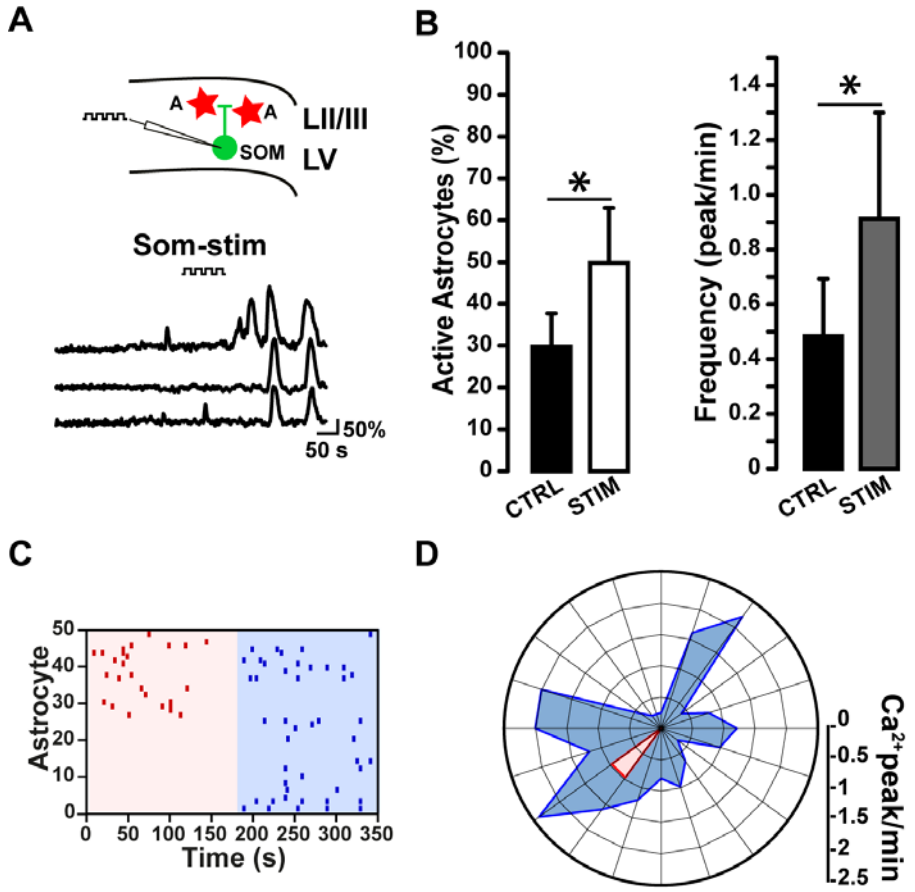

Figure 17. Stimulation of a single SOM interneuron evokes astrocytic Ca^{2+} events. (A) Schematic experimental representation (upper panel) showing the patch pipette to selectively stimulate a SOM expressing interneuron in LV, while performing Ca^{2+} imaging from astrocytes loaded with Rhod-2 AM in LII/III (red stars). In the lower panel the time course of Ca^{2+} changes in three astrocytes from SSCx L2-3 before, during and after induction of action potential firing in a single SOM cell. (B) Summarizing histograms showing the percentage of active astrocytes and the mean Ca^{2+} peak frequency before and after the stimulation of a single SOM interneuron. The application of $GABA_B$ receptor antagonist almost completely abolished the astrocytes Ca^{2+} activity (75 astrocytes, 5 experiments, 3 animals; for percentage p= 0.03, for frequency p= 0.019, *p<0.05, **p<0.01, *** p<0.001). (C) Raster plots of Ca^{2+} peaks over time for all astrocytes monitored. The red area represent basal Ca^{2+} activity with some astrocytes exhibiting spontaneous Ca^{2+} oscillations, while the blue area represents Ca^{2+} activity after SOM single cell stimulation. (D) Radar plot of the Ca^{2+} peak frequency before (red) and after (blue) stimulation of a SOM interneuron. Radii represent only astrocytes showing an increase in Ca^{2+} peak frequency and circles represent the Ca^{2+} frequency value.

3.6 GABA-activated astrocytes modulate pyramidal neuron excitability

We next investigated whether and how GABA activated astrocytes signal back to neurons. We applied Bac while performing single or dual cell patch-clamp recordings from pyramidal neurons in SSCx slices in the presence of TTX (1μM). To avoid a sustained activation of $GABA_B$ receptors which is known to induce in neurons slow, long lasting inhibitory currents, we used instead of bath perfusion, brief (400-600 ms) local applications with Bac that induced, in most neurons tested, slow postsynaptic $GABA_BR$-mediated outward currents (I_{out}) with a mean duration of 54 ± 9 s (Fig. 18 C, n= 10 out of 15); the duration was dependent on the distance between the neuronal soma and the Bac application site that was between 80 and 150 μm. Bac also evoked large amplitude, oscillatory Ca^{2+} transients in astrocytes (Fig. 10 D). We found that Bac applications significantly increased the frequency of slow inward currents (SICs) that occurred both during and after the evoked I_{out} in the 2 minutes following Bac applications. Both spontaneous and Bac-induced SICs had similar slow kinetics (rise 10-90 %: 94 ± 16 ms, n= 60, before and 99 ± 10 ms, n= 98, after Bac, p= 0.248; decay 90-10 %: 440 ± 111 ms, n= 57, before and 333 ± 29 ms, n= 95, after Bac, p= 0.123; duration: 0.79 ± 0.10 s, n= 59, before and 0.98 ± 0.10 s; n= 93, after Bac, p= 0.203), but peak amplitude and area of Bac-induced SICs were significantly increased with respect to spontaneous SICs (Fig. 18 C). Both spontaneous and Bac-induced SICs and were mediated by NMDA receptors, being completely blocked by D-AP5 (50 μM; not shown).

To assess whether Bac-evoked SICs depend on astrocytic Ca^{2+} oscillations, we performed patch-clamp experiments in slices from $IP_3R2^{-/-}$ mice in which G-protein coupled Ca^{2+} elevations are impaired in astrocytes, as reported above (Fig. 12 A). We found that in slices from $IP_3R2^{-/-}$ mice Bac failed to increase SICs frequency, amplitude and charge in pyramidal neurons (n = 13; Fig. 18 A, C). These data indicate that the increased frequency of SICs observed in neurons upon Bac challenge is mediated by astrocytic Ca^{2+} elevations.

In the cortical and hippocampal regions Ca^{2+} elevations mediated by mGluRs in astrocytes lead to glutamate release that induced SICs in neighbouring pyramidal neurons. Pair recording and Ca^{2+} imaging experiments also revealed that SICs can synchronize small groups of contiguous pyramidal neurons [30].

We thus tested if Bac-evoked SICs also induce synchronization of pyramidal neuron activity. To this aim, we performed patch-clamp recordings from pairs of pyramidal neurons at different distances to each other. When pyramidal

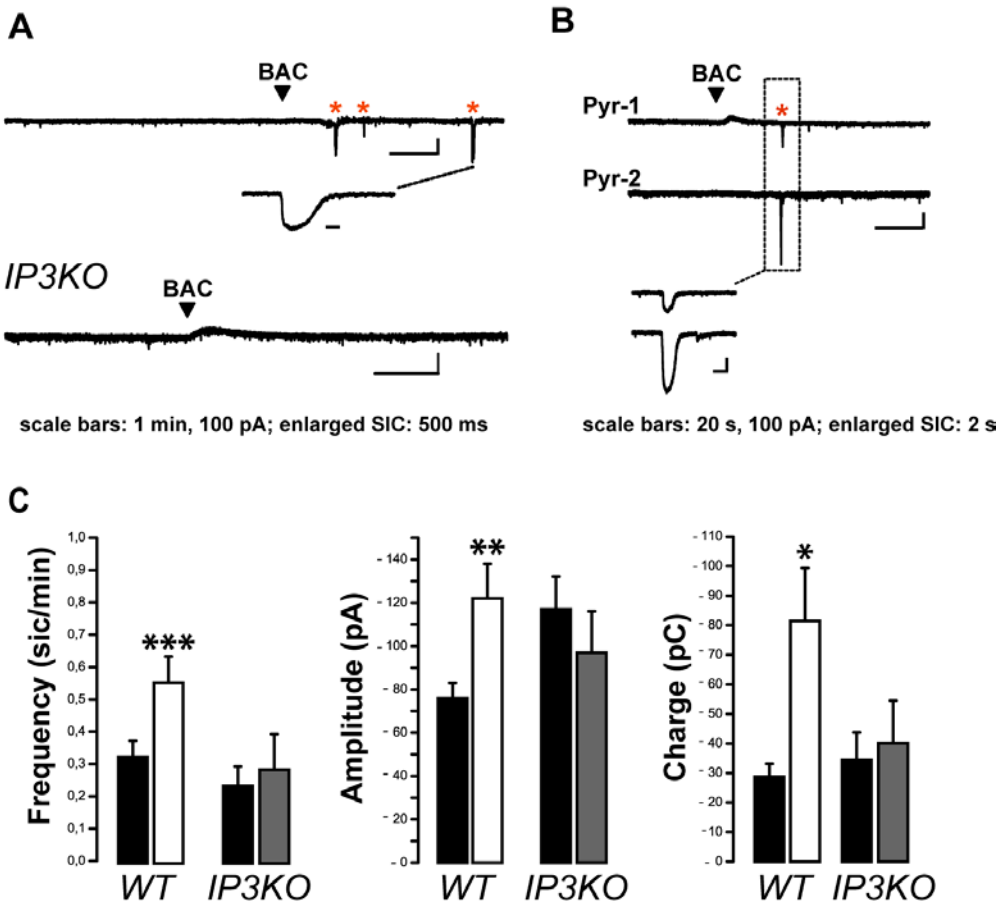

Figure 18. GABA-activated astrocytes evoked slow inward currents (SICs) in pyramidal neurons.
(A) Representative whole cell currents of a pyramidal neurons (Pyr) showing the occurrence of SICs (red asterisks) after local application of Baclofen (BAC, black arrowhead) in SSCx, LV from WT mice (upper trace) but not in a pyramidal neuron from an IP_3R2 KO mice (lower trace; scale bars: 1 min 100 pA; enlarged SIC: 500 ms). (B) SICs can occur synchronously in adjacent pyramidal neurons 100 µm apart (scale bars: 20 s, 100 pA; enlarged SIC: 2 s). (C) Summary of SICs mean values before (5 minutes) and after (3 min) local application of Baclofen in WT and IP_3R2 knock-out mice. Frequency, wild type, n= 21 cells; 12 animals; p= 0.001; paired Student's t test; IP_3R2 knock out, n= 13 cells; 5 animals; p= 0.972; paired Student's t test. Amplitude, wild type, n= 62 and 57 SICs for control and BAC respectively; p=0.007; unpaired Student's t test; IP_3R_2 knock out, n= 30 and 15 SICs for control and BAC respectively; p=0.434; unpaired Student's t test. Charge transferred, wild type, n= 60 and 52 SICs for control and BAC respectively; p= 0.009; unpaired Student's t test; IP_3R2 knock out, n= 30 and 15 SICs for control and BAC respectively; p= 0.724; unpaired Student's t test. Recordings at Vh= -70 mV; in zero Mg^{2+}, TTX 1 µM. SICs kinetics: Rise time: 94 ± 13 ms (n= 60) before and 69 ± 7 ms (n= 100; all events) after Bac (p= 0.058).

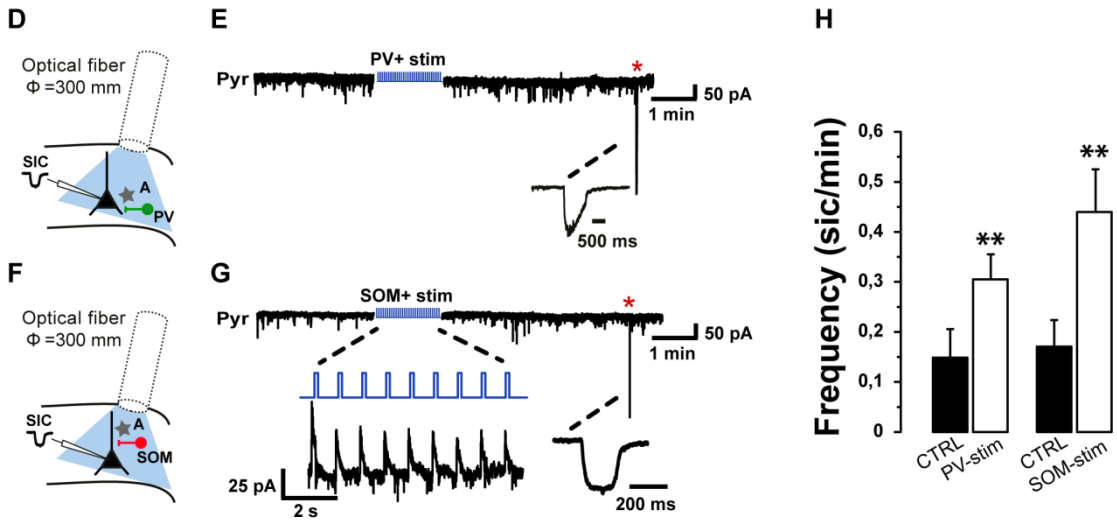

Figure 18. PV and SOM interneuron stimulation evoke SICs-like activity in pyramidal neurons.
(D, E) Schematic representation of the experimental set up for optogenetic experiments showing the optical fiber used to deliver blue light (see Fig 14 and 16) for selective stimulation of PV (green) or SOM (red) interneurons expressing ChR_2, while recording in voltage clamp from a pyramidal cell (black). (F, G) Whole cell recording of a pyramidal neuron (Pyr) before, during and after the photo-stimulation of PV or SOM interneurons (blue stepped lines). Recordings at Vh= -70 mV; in 0.5 Mg^{2+}, without TTX. (H) Summarizing histogram of the mean frequency, amplitude and charge transferred of SICs before (5 minutes) and after (5 minutes) blue light stimulation of the selected interneuron population (PV stimulation, n= 6 cells, 4 animals; SOM stimulation, n= 6 cells, 5 animals p= 0.01); *p<0.05, **p<0.01, *** p<0.001.

neurons were <100 μm apart, 12 out of 35 Bac induced SICs were synchronous (<100 ms, range 4÷74 ms from 2 paired recordings), while in pyramidal neurons that were ≥100 μm apart, only 2 out of 48 Bac-induced SICs were synchronous (3 paired recordings; Fig. 18 B).

Finally, we tested whether astrocyte Ca^{2+} transients induced by optogenetic stimulation of ChR_2 expressed in PV or SOM interneurons could also evoke SICs-like in pyramidal neurons. We performed patch-clamp recordings from pyramidal neurons in SSCx while stimulating with blue light ChR_2-expressing interneurons and found that SICs frequency increased significantly after light stimulation (Fig. 18 D-H).

3.7 Ongoing experiments: modulation of network activity by GABA-activated astrocytes

We are currently investigating whether GABA-activated astrocytes modulate local network activity and neuronal synchronization. In SSCx slices we recorded UP states from pyramidal neurons before and after local Bac applications (100 μM). We found that Bac determines a significant increase in Up state duration in WT mice, but not in IP_3R2 KO mice, indicating that Bac effect was mediated by astrocytic Ca^{2+} responses. In IP_3R2 KO mice the duration tended to decrease and the frequency was significantly reduced after Bac (Fig. 19 A, B, C). These preliminary data suggests that GABA-activated astrocytes positively modulate local network activity by increasing the duration of UP states and that the Ca^{2+} transients mediated by IP_3R2 in astrocytes are necessary for the modulation of local synchronous activity.

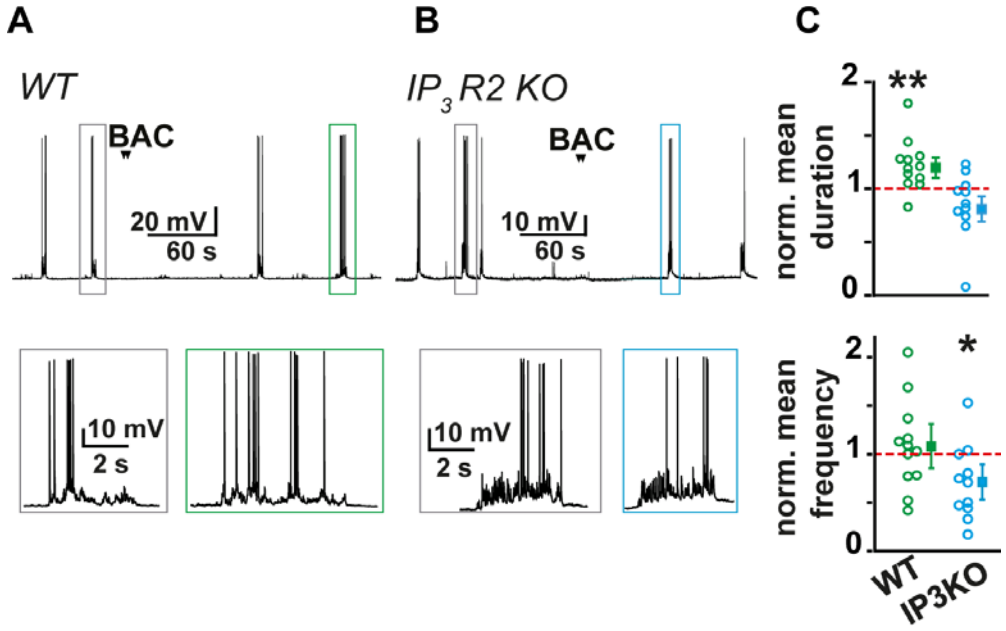

Figure 19. Modulation of network activity by GABA activated astrocytes. (A, B) Whole cell current clamp recordings of spontaneously generated states (i.e. UP states) in somatosensory cortex LV pyramidal neurons before and after double pressure application of baclofen (100 μM) from WT (A) and IP_3R2 KO mice (B). Representative UP states are showed at enlarged time scale. (C) Distribution of normalized mean durations of UP states in WT and IP_3R2 KO mice. D) Distribution of normalized mean frequency of UP states in WT (13 cells, 7 animals; for duration, p= 0.004; for frequency p= 0.360) and IP_3R2 KO mice (12 cells, 6 animals; for duration, p= 0.166; for frequency, p= 0.024); *p<0.05, **p<0.01, *** p<0.001.

4. Discussion and conclusions

In the present study we identified a novel signalling circuit between cortical interneurons and astrocytes. We demonstrated that two main classes of inhibitory interneurons, i.e., PV- and SOM-expressing interneurons, differently recruit neighbouring astrocytes via GABAergic transmission. Cortical astrocytes close this circuit by releasing glutamate and converting a transient inhibition into a prolonged excitation of neighbouring pyramidal neurons. Specifically, we unveiled three hallmarks of the communication between interneurons and astrocytes in the neocortex. Firstly, we demonstrated that cortical astrocytes respond with Ca^{2+} oscillations to exogenous GABA applications, both in brain slice and *in vivo* preparations, and that this activation is mediated by $GABA_B$ receptors. Secondly, we showed that astrocytes respond with complex Ca^{2+} signals to the selective activation of SOM- and PV-expressing interneurons. Astrocytes are highly sensitive to GABA released from SOM interneurons and also exhibit long-term plastic changes in their Ca^{2+} response to intense activity of SOM, but not PV interneurons. Finally, we proved that $GABA_B$ receptor-activated astrocytes respond to interneuron activation by releasing the gliotransmitter glutamate.

4.1 Mechanism of GABA sensitivity in cortical astrocytes

In an initial series of experiments in cortical slices obtained from young mice, we observed that about 60 % of cortical astrocytes showed intense somatic Ca^{2+} transients in response to bath or local perfusion with GABA. This response was replicated with $GABA_B$ receptor, but not with $GABA_A$ receptor agonists. These findings demonstrate that cortical astrocytes respond to GABA specifically through $GABA_B$ receptor-mediated Ca^{2+} increases. Our results are consistent with previous studies reporting that GABA-induced Ca^{2+} elevations in hippocampal astrocytes are mediated by $GABA_B$ receptors [34,81,83]. To explain hippocampal astrocyte sensitivity to GABA, an additional mechanism has been proposed that involves the depolarization of the astrocytic membrane mediated by $GABA_A$ receptor and activation of voltage-sensitive Ca^{2+} channels (VOCCs) [83]. A possible explanation, of this apparently conflicting, results

relies on the different expression of $GABA_A$ receptors, $GABA_B$ receptors or VOCCs in astrocytes from the cortex or hippocampus. However, it has been demonstrated that astrocytes, in both the neocortex and the hippocampus, express $GABA_B$ receptors that are localized in processes surrounding both glutamatergic and GABAergic synapses [131,132]. $GABA_A$ receptors are also abundantly expressed in astrocytes throughout brain regions [133]. Conversely, it is not well established if mature astrocytes express VOCCs. Indeed, the presence of VOCCs is confirmed only in astrocyte cultures after trophic manipulations [134,135]. Experiments in mature astroglial cells in situ do not demonstrate measurable VOCCs currents, and there are only few examples of up regulation of L- and P/Q channels in cells undergoing reactive astrogliosis in status epilepticus [134,136]. However, cultured astrocytes, in terms of the general behavior and receptor expression, are not considered a faithful model of astrocytes in the intact brain. Because in our experimental conditions cortical astrocytes did not respond to Mus with intracellular Ca^{2+} increase, we argue that this $GABA_A$ mediated activation of VOCCs is unlikely to occur in cortical astrocytes.

The third mechanism for GABA-induced Ca^{2+} elevations in astrocytes has been revealed in the olfactory bulb and it involves GABA transporters and the Na^+/Ca^{2+} exchanger [85]. However in our experiments $GABA_B$ antagonists completely abolished GABA-mediated Ca^{2+} elevations suggesting that this mechanism does not significantly contribute to GABAergic responses in cortical astrocytes.

4.2 Long lasting responses in astrocytic processes

We took advantage of $GCaMP_3$::GLAST-CRE transgenic mice to study GABAergic responses at the level of thin astrocytic processes. This approach offers a consistent advantage over bulk loading with synthetic calcium dyes that achieve good signal-to-noise ratio only in somatic and perisomatic astrocytic processes. As never reported before, we found that local brief applications with GABA or $GABA_B$ receptor agonists could evoke prolonged and intense Ca^{2+} transients in astrocytic branches. The local release of GABA in the proximity of a single process, determined complex intracellular Ca^{2+} dynamics. Some events

were local and restricted only to few μm^2 subregions, while others invaded expanded domains, spreading over whole processes and eventually the soma. These results support the view that astrocytic processes are key sites of neuron-astrocyte signalling. Indeed, astrocytic processes contact different neuronal sites and are the site where neuronal signals are integrated in space and time. Indeed, neuronal information may be encoded into the dynamic Ca^{2+} changes that either remain spatially restricted to individual and multiple processes or recruit the entire astrocyte in a global Ca^{2+} response [26,27]. The molecular mechanism responsible for the observed long-lasting Ca^{2+} oscillations in astrocytes remains undefined. A candidate mechanism is the release of gliotransmitters from activated astrocytic processes, such as glutamate and ATP. These gliotrasmitters can, in turn, act on both astrocytic and neuronal receptors. Several studies demonstrated that astrocytes deploy a purinergic extracellular signalling system. Cultured astrocytes can release ATP upon diverse stimuli and, in turn, respond to ATP with Ca^{2+} elevations indicating a sort of autocrine cell stimulation mechanism [137]. Evidence from hippocampal slices revealed a combined release of glutamate and ATP from stratum radiatum astrocytes during electrical neuronal simulation. This release initiated a wave of astrocyte activation mediated by ATP acting on P2Y1 astrocytic receptors which promoted Ca^{2+} release from intracellular Ca^{2+} stores by the activation of the IP_3 production cascade [123]. Nonetheless, further investigations are needed to fully understand this mechanism.

4.3 Astrocytic $GABA_B$ intracellular cascade

Neuronal $GABA_B$ receptors are coupled to $G_{i/o}$ proteins that mediate both pre- and postsynaptic effects, mainly by inhibiting voltage-gated Ca^{2+} channels and by activating potassium channels, respectively [84]. Instead, the mechanism at the basis of the intracellular Ca^{2+} transients mediated by $GABA_B$ receptor activation is undefined.

We started to dissect the intracellular signalling cascade that leads to $GABA_B$ receptor-mediated intracellular Ca^{2+} elevations in astrocytes. Our results from the experiments that used pertussis toxin and those in IP_3R2 KO mice clearly indicate that both $G_{i/o}$ proteins and IP_3 receptor signalling are necessary for

$GABA_B$-mediated Ca^{2+} responses in astrocytes. However astrocytic Ca^{2+} oscillations generally result from activation of the G_q-coupled metabotropic receptor and IP_3 intracellular signalling cascade. In addition, it is not known if $G_{i/o}$ proteins signalling converge on the IP_3 receptor signalling pathway. Activation of $G_{\beta/\gamma}$ proteins may lead to stimulation of PLC_β1-3 [138] or directly of IP_3 formation [139]. Alternatively, a specific interaction between $G_{i/o}$ and G_q protein could also account for the evoked IP_3R2-dependent Ca^{2+} transients in astrocytes. Nevertheless, the characterization of the full signalling $GABA_B$ receptor intracellular pathway in astrocytes goes beyond the scope of this study.

4.4 Astrocyte GABAergic responses in adult mice

Our study provides the first demonstration that astrocytes from layer II/III respond with Ca^{2+} elevations to the inhibitory neurotransmitter GABA. This result validates our extensive measurements of astrocyte responsiveness to GABA in brain slice preparations both from young and adult mice. Effectively, we observed that the astrocyte response, both in terms of Ca^{2+} peak frequency and number of responsive astrocytes was reduced *in slice* preparations from adult mice with respect to that obtained from young mice as well as from *in vivo* experiments in adult mice, demonstrating that the GABAergic signalling on astrocytes is only weakly developmentally regulated. This results contrast with previous findings in the hippocampal slices, where Meier and colleagues (2008, [83]) reported that the Ca^{2+} response mediated by $GABA_B$ receptors in astrocytes was age-dependent. The reasons for this discrepancy are unclear, but may be linked to the different brain areas investigated. Notably, the experiments reported in Meier et al. were limited to slice preparations. As the brain tissue from adult animals is more sensitive to slicing procedures, only a limited number of astrocytes may survive in brain slices from adult mice thereby explaining the reduced GABAergic response of astrocytes in this preparation. Further characterization of the developmental expression profile of $GABA_B$ receptors from astrocytes in different brain areas appears necessary to fully understand how the interactions between specific interneuron subclasses and astrocytes evolves during the maturation of cortical circuits.

4.5 PV and SOM interneuron specific signalling to astrocytes

It is widely accepted that clarifying interneuron diversity and its functional consequences is critical to understanding information processing within the cerebral cortex. For instance, PV and SOM GABAergic interneurons differentially control the inputs and outputs of the network thanks to their differential firing properties and their targeting to specific domains of pyramidal neurons and other interneurons [55,56,3].

In our study we demonstrated, for the first time, that PV and SOM interneurons interact differently with cortical astrocytes. By means of optogenetic activation of interneuron population or activation of individual cells by intracellular current pulses, we were able to dissect out the specific signalling to astrocytes of LII/III and LV PV or SOM interneurons.

Firstly, we showed that SOM interneurons were more efficient than PV interneurons in recruiting downstream astrocytes, both in terms of Ca^{2+} peak frequency and number of activated astrocytes. Secondly, we observed long-term changes in Ca^{2+} elevations evoked in astrocytes by SOM but not PV interneuron stimulation indicative of a specific plastic response of astrocytes to GABA released from SOM interneurons. Indeed, we found that the Ca^{2+} response of astrocytes was significantly larger to the second with respect to the first light activation of SOM interneurons, while the astrocytes response to similar repetitive activation PV interneurons was either unchanged or eventually reduced. .Thirdly, the recruitment of astrocytes by PV or SOM interneurons led to different network activity modulation. After the specific stimulation of SOM interneurons, astrocytes recruitment was greater and the SIC-like events recorded in pyramidal cells were recorded at higher frequency than that observed after PV interneuron stimulation.

A possible functional explanation for the differences in the astrocyte response to SOM and PV interneurons relies on the distinct role of these two interneuron populations: the axonal projections of SOM interneurons target the distal dendrites of pyramidal neurons providing a fundamental contribution to signal integration, while those from PV interneurons target mainly the soma and proximal dendrites exerting a tight control of the spiking behaviour of these cells. The prompt response of astrocytes to SOM interneurons and the plasticity

of their response suggest that astrocytes activated by GABA may exert a modulatory control of excitatory synaptic transmission that target distal dendrites of pyramidal neurons. In this framework, astrocytes appear to be, therefore, targets not only of excitatory but also of inhibitory signals. How astrocytes respond to this dual, possibly conflicting, signal remains to be defined. However, our results suggest that GABA-activated astrocytes may turn a transient, though intense episode of GABAergic transmission into a delayed, possible long-lasting change in local circuit excitability. It is here that astrocytes not only communicate with SOM inhibitory synapses, but also with hundreds of excitatory inputs contacting neuronal dendrites [140,11,141]. In turn, SOM activated-astrocytes release glutamate that is more effective in depolarizing its neuronal targets, as neuronal dendrites are rich in excitatory spines and extrasynaptic NMDARs. This can be important for modulating dendritic integration at a longer temporal scale after SOM signalling has ceased.

On the other hand, astrocytes receiving PV input reside in somatic layers, where PV perisomatic inhibition needs to tightly regulate, like a clockwork, the neuronal firing rather than being plastic [142]. Accordingly, these astrocytes are likely to interact with fewer synapses, given that excitatory inputs are usually rare around the soma, and are consequently less responsive.

4.6 Neuronal network modulation by GABA-activated astrocytes

We found that GABA-activated astrocytes release glutamate and trigger NMDA receptor-mediated SICs in pyramidal cells. Our results demonstrate that astrocytes are not just passive listeners of GABAergic activity, but can also signal back to the neuronal network. Therefore, we propose that astrocyte can turn a strong inhibitory input into a delayed excitation of the network. In particular, we speculate that glutamate release from GABA-activated astrocytes represent a mechanism for neuronal synchronization. Synchronization of neuronal activity is hypothesized to be of fundamental relevance to information processing in the brain [143]. Together with the GABA sustained Ca^{2+} activity in astrocytes, GABA evoked SICs occurred for several minutes, outlasting the time of GABA agonist applications, and were longer than spontaneous ones. According with observations by Fellin and colleagues (2004, [30]), the

synchronization of SICs could derive from a single episode of astrocytic glutamate release that activates extrasynaptic NMDARs from the adjacent dendrites of neurons. Indeed, in paired recordings we observed that Bac could trigger SICs synchronous in pyramidal cells 100 μm apart. This means that glutamate released from astrocytes can synchronize the activity in adjacent neuronal domains. In support to this hypothesis, our preliminary data indicate that GABA-activated astrocytes have the potential to positively modulate the duration of cortical UP states responsible of slow cortical oscillations. UP states involve high-frequency firing activity that occurs synchronously in clusters of neurons, including GABAergic interneurons [144]. It is possible that GABA released during UP states activates astrocytic responses. Notably, our data from IP_3R2-KO mice, where Ca^{2+} signalling is impaired in astrocytes, reveal opposing effect of $GABA_B$ receptor activation on UP state duration. In these mice, Bac reduced both duration and frequency of cortical UP states. This suggests that when astrocytes are activated by Bac, as in WT mice, they are able to induce a delayed increase in network activity underlying UP states despite the direct inhibitory effect of Bac on neurons [145,146]. Although additional experiments are needed to clarify this issue, we suggest that astrocytes contribute to set local circuit excitability and to regulate brain network states.

4.7 Conclusions

In my doctorate Thesis I propose a view where GABAergic interneurons, and SOM interneurons in particular, can have a double impact on network activity. Firstly, they can directly inhibit neuronal elements. Secondly, they can activate local astrocytic processes and stimulate gliotransmission. Specifically, in response to a strong inhibition astrocytes may release glutamate. The release of glutamate from astrocytes has several physiological implications. At a single cell level, it can modulate synaptic integration. For instance, an increased level of glutamate release onto pyramidal cell dendrites has been shown to extend the spatio-temporal window of synaptic integration by lowering the threshold of NMDA-triggered dendritic regenerative events [147]. At the level of local circuits, the simultaneous depolarization of neighbouring neurons by SICs can

play a role in the transition between synchronous and asynchronous brain states. As an extreme example, glutamate release from GABA-activated astrocytes could play a role at the onset of epileptic seizures, which constitutes the most dramatic brain state transition. Indeed, before epileptic seizures, inhibitory interneurons fire at high rates but they often fail to constrain the abnormal activity of excitatory cells [148]. The release of glutamate from astrocytes might fuel the synchronous firing from excitatory neurons and favour seizure initiation.

5. Materials and methods

Animal strains. The mice used in this study were of mixed backgrounds (c57bl6, CD-1) and sexes. All procedures were conducted in accordance with the Italian and European Communities Council Directive on Animal Care and were approved by the Italian Ministry of Health. Mice were used at postnatal days 15-20 (P15-20; young) and P35-60 (adults). Transgenic mice used were: Tg(*Gad*GFP)45704Swn (GIN; SOM cells), Tg(*Gad1*-EGFP)G42Zjh (G42; PV cells), *Gt(ROSA)26Sor*<tm14(CAG-tdTomato)Hze> (ROSA-tdTomato), *Pvalb*<tm1(cre)Arbr> (PV-Cre), *Sst*<tm2.1(cre)Zjh> (SOM-Cre), IP_3R2 KO. The $GCaMP_3$::GlastCreERT2 line was obtained crossing the $GCaMP_3$ (B6;129S-*Gt(ROSA)26Sortm38(CAG-GCaMP3)Hze*/J) and a GlastCreERT2 [149]. The expression of $GCaMP_3$ was tamoxifen inducible. Tamoxifen (SIGMA Aldrich, Milano, IT) was dissolved in corn oil (SIGMA Aldrich, Milano, IT) at 37°C for 5 hours to prepare the 20 mg/ml stock solution. Tamoxifen was injected intraperitoneally with a protocol depending on the age of the animals: 1 mg/day administered in two injections repeated for two days (P7 to 10) for young mice and for five days (P30 to 35) for adult mice. Mice that received tamoxifen were analyzed 7/10 days after the last tamoxifen-injection. Except for IP_3R2 KO and for $GCaMP_3$::GlastCreERT2 lines, animals used for experiments were heterozygous for the indicated genes.

Brain slice preparation.

Slicing. Coronal neocortical slices of 350 μm were obtained from mice at postnatal days P15-20 and P30-60. Animals were anaesthetized with Zoletil (40 mg/kg) and Xilazyne (40 mg/kg) and the brain was removed and transferred into an ice-cold solution (ACSF, in mM: 125 NaCl, 2.5 KCl, 2 $CaCl_2$, 1 $MgCl_2$, 25 glucose, pH 7.4 with 95% O_2 and 5% CO_2). Coronal slices were cut with a vibratome (Leica Vibratome VT1000S Mannheim, Germany) in the solution described in Dugue et al., 2005. Slices were transferred for 1 minute in a solution at room temperature (in mM, 225 D-mannitol, 2.5 KCl, 1.25 NaH_2PO_4, 26 $NaHCO_3$, 25 glucose, 0.8 $CaCl_2$, 8 $MgCl_2$, 2 kynurenic acid with 95% O_2 and 5% CO_2). Finally, slices were transferred in sACSF at 30°C for 20 min and then maintained at room temperature for the entire experiment.

Dye loading. Slices were kept in ACSF with Sulforhodamine 101(SR101) (0.1 µM, Sigma Aldrich, Milano) at 30°C for 15 min to selectively stain astrocytes before the Ca^{2+} dye loading. Next slices were recovered for 15 min at 31°C and loaded with the Ca^{2+} sensitive dyes Fluo-4 AM or Rhod-2 AM (10 µM; Life Technologies, Monza, IT). Loading was performed in a ACSF solution containing sulfinpyrazone (200 µM, Sigma Aldrich, Milano, IT; to limit the secretion of the fluorescent dye in its free acid form), pluronic F-127 (0.12%, Sigma Aldrich, Milano, IT; to prevent fluorescent dye aggregations), and kynurenic acid (1 mM, Sigma Aldrich, Milano, IT; to reduce glutamate excitotoxicity) and constantly bubbled with 95% O_2 and 5% CO_2. With this procedure mostly astrocytes are loaded with the dye, while neurons remain unstained (only the 5% of total neurons was marked).

Pertuxis toxin application. Slices from $GCaMP_3$::GlastCreErt2 mice were loaded with SR101. For each slice one hemisphere was incubated in ACSF containing PerTx (7.5 µg/ml, SIGMA Aldrich, Milano, IT) for 3 to 5 hours. Then brain slices were continuously perfused with the same solution in a submerged chamber (Scientifica, UK) at a rate of 4 ml min^{-1} with 5% CO_2/95% O_2 for 1 hour. The other hemisphere was incubated in ACSF alone and used for control experiments.

Drugs application. Drugs applied in bath perfusion were GABA 200 µM (Tocris, Bristol, UK); Baclofen 20-50 µM (Tocris, Bristol, UK); SCH50911 20-50 µM (Tocris, Bristol, UK), CGP52432 20 µM (Abicam Biomedicals, UK), Muscimol 100 µM (Tocris, Bristol, UK), Picrotoxin 100 µM (SIGMA Aldrich, Milano, IT), DHPG 20-50 µM (Tocris, Bristol, UK), Tetrodotoxin 1 µM (Abcam, Cambridge, UK). Drugs applied by a glass pipette with a resistance of 2.5 MΩ controlled by pressure ejection unit (PDES, NPI Electronics, Tamm, Germany; 3 psi; 200÷500 ms) were: GABA 500 µM; Baclofen 500 µM, DHPG 500 µM.

Ca^{2+} imaging.

Slice imaging experiments were conducted with a confocal laser scanning microscope TCS-SP5-RS (Leica Microsystems, GmbH, Wetzlar, Germany) equipped with two solid state lasers tuned at 470 nm and 550 nm to image the astrocytes somatic Ca^{2+} variation in brain slices from young animals. To image the Ca^{2+} dynamics in astrocytic processes or in soma from adult mice we

deployed a two photon laser scanning microscope Multiphoton Imaging System (Scientifica Ltd., Uckfield, East Sussex, United Kingdom) equipped with a pulsed infrared laser (Chameleon Ultra 2,Coherent) tuned at 910 nm. Power at sample was controlled in the range 5-10 mW. The excitation wavelengths used were: 470 nm or 740 nm for Fluo-4 AM, 550 nm for Rhod-2 AM and 470 nm or 910 nm for $GCaMP_3$. SR101 is visible both at 740 nm and 910 nm. Images were acquired with a water-immersion lens (Olympus, LUMPlan FI/IR x20, 1.05 numerical aperture (NA)) at a resolution of 512x512 with zoom 2 or 4 at 1-2 Hz frame rate. Imaging was performed in cortical layers 2-3 and 5 and conducted for at least 1 h with an interval of 5 min for each slice.

In vivo imaging experiments were performed on $GCaMP_3$::GlastCreERT2 mice between postnatal days 30-60. Mice were anaesthetized with an intraperitoneal injection of urethane (20% urethane, ethylcarbamate; SIGMA Aldrich, Milano, IT) solved in saline solution (0.8 ml/hg). Animal pinch withdrawal and eyelid reflex were tested to assay the depth of anaesthesia. Dexametasone sodium phosphate (2 mg/kg body weight) was injected intramuscularly to reduce cortical stress response during surgery and prevent cerebral edema. Dextran trich (20 µl; Sigma Aldrich, Milan, IT) was injected in caudal vein to selectively mark blood vessel. We monitored the respiration rate, heart rate, and core body temperature throughout the experiment. The mouse was head-fixed and a craniotomy of 2–3 mm in diameter was drilled over the somatosensory cortex. Mice were mounted under the microscope with a metal head-post glued to the skull. The two-photon microscope (Ultima IV, Prairie Technology now Bruker, USA) was equipped with a pulsed infrared laser (Chamaleon Ultra 2,Coherent, Santa Clara, CA, USA) and tuned at 910 nm (to co-excite $GCaMP_3$ and Dextran Tritc) that delivered about 30 mW at the sample. Imaging was performed through a water-immersion lens (x60, 0.98 numerical aperture (NA) Olympus, LUMPlan FL/N) at a resolution of 512x512 pixels with zoom 4, leading to a field of 50.7x50.7 µm in superficial layers (50-150 µm below the cortical surface) and acquired at 1-2 Hz. Imaging session lasted up to 2h.

Virus injection. Adeno-associated viruses (AAVs) for ChR_2 were acquired from the University of Pennsylvania Viral Vector Core: AAV2/1.EF1.dflox.hChR2(H134R)-mCherry.WPRE.hGH (Addgene 20297) or

AAV yfp. Newborn mice (P0–P2) were anaesthetized on ice and secured into a molded platform. ChR_2 virus was injected into pups of PV-Cre and SOM-Cre mice crossed to various GFP transgenic lines at the IIT facilities. The stereotaxic coordinates for SSCx were 0 mm posterior to Bregma, 1.5 mm lateral to sagittal sinus and 0.150 mm depth. After injections the skin was sutured and pups were revitalized under a heat lamp and returned to their cage.

Optogenetic experiments. Full-field photo-stimulation of ChR2-expressing interneurons consisted of a train of light pulses (150 ms at 1-2Hz for 1 min) delivered by a 5-W blue LED (Thorlabs LEDC5), which was collimated and coupled under the objective with an optic fiber (ThorLabs, Newton, NJ, USA) held at 26 degrees angle. The optic fiber was 350 µm in diameter with a 0.22 NA. The resulting illuminated ellipse was 550 µm for 150 µm in diameter. The led was directly controlled by a command voltage with a TTL signal.

Electrophysiological recordings. Brain slices were continuously perfused in a submerged chamber at a rate of 3-4 ml min^{-1} with (in mM): NaCl, 120; KCl, 2.5; NaH_2PO4, 1; $NaHCO_3$, 26; $MgCl_2$, 1; $CaCl_2$, 2; glucose, 10; at pH 7.4 (with 5% CO_2/95% O_2). Neurons were visualized under a microscope (TCS-SP5-RS, Leica Microsystems, GmbH, Wetzlar, Germany or Multiphoton Imaging System, Scientifica Ltd., Uckfield, East Sussex, United Kingdom) equipped with a CCD camera for differential interference contrast (DIC) image acquisition. Single and dual cell recordings were performed in voltage-clamp and current-clamp configuration using a multiclamp-700B amplifier (Molecular Devices, Foster City, CA, USA). Signals were filtered at 1 kHz and sampled at 10 kHz with a Digidata 1440s interface and pClamp10 software (Molecular Devices, Foster City, CA, USA). Typical pipette resistance was 3–4 MΩ. Access resistance was monitored throughout the recordings and was typically <25 MΩ. Whole-cell intracellular pipette solution was (in mM): K-gluconate, 145; $MgCl_2$, 5; EGTA, 0.5; Na_2ATP, 2; Na_2GTP, 0.2; HEPES, 10; to pH 7.2 with KOH, osmolarity, 280÷290 mOsm (calculated liquid junction potential: -14 mV) prepared using RNase-free water and salts. Data were not corrected for the liquid junction potential. *Pyramidal cells* were identified on the basis of their distinct morphology characterized by the triangular shape of the soma, a main apical dendrite pointing towards the *pia* and the absence of a main dendrite in the

opposite direction. Their biophysical identity was confirmed by their response to hyperpolarizing and depolarizing 750 ms current steps. In particular, regular spiking pyramidal neurons showed a firing discharge with no spike amplitude accommodation (except for the second action potential in some cells), small after hyperpolarization and low steady-state frequency (15÷23 Hz with 200 pA current injection). *ChR_2-positive PV interneurons* (PV) were identified by fluorescence and their biophysical identity was confirmed by high steady-state firing frequency (50÷90 Hz with 400 pA current injection), no spike amplitude accommodation nor frequency adaptation and large afterhyperpolarization. *ChR_2-positive SOM interneurons* (SOM) were identified by fluorescence and their biophysical identity was confirmed by a clear sag, one or more rebound action potentials, spike amplitude accommodation and frequency adaptation and large biphasic afterhyperpolarization.The following parameters were measured to characterize passive membrane properties: resting membrane potential (V_{rest}) was recorded immediately after the rupture of the neuronal membrane; input resistance (R_{in}) was determined by measuring the voltage change in response to a small hyperpolarizing and depolarizing current pulses (±50 pA, 750 ms) at resting potential. All patched neurons were from cortical layer 2-3 and 5. All pyramidal neurons were voltage-clamped at -70 mV. Slow inward currents (SICs) were recorded in Mg^{2+} free solution in presence of tetrodotoxin (TTX, 1 μM; Abcam, Cambridge, UK).

Data analysis. Data analysis was performed with Clampfit 10, Origin 8.0 (Microcal Software), Microsoft Office, ImageJ (NIH) and MATLAB 7.6.0 R2008A (Mathworks, Natick, MA, USA).

Ca^{2+} analysis. Image sequences were aligned and processed with ImageJ and MATLAB custom software. Region of interests (ROIs) were manually drawn around cellular somata and processes using the red channel from the SR101 signal. All pixels within each ROI were averaged to give a single time course F(t). To compare relative changes in fluorescence between different cells, the Ca^{2+} signal for each ROIs was expressed as $\Delta F/F_0=(F(t)-F_0)/(F_0\text{-background})$, where F_0 is the baseline fluorescence level obtained by averaging the fluorescence recorded during baseline activity. A fluorescence increase was considered significant event when exceeding three fold standard deviation from

the baseline. Astrocytic processes were analyzed in MATLAB as previously described [26]. Briefly, astrocytic processes were segmented in 1μm^2 subregions. F(t) from each subregion were divided by the corresponding SR101 signal to correct for minor, transient *z* motions. *x-y* drifts were automatically corrected off-line; cells experiencing a *z* drift were discarded. All detected Ca^{2+} events were automatically reported in a raster plot and in a radar plot checked by the operator. All results are presented as mean ± s.e.m. Statistical analyses were performed with two-tailed paired Student's *t*-test. Results were considered statistically significant when *p<0.05, **p<0.01, *** p<0.001.

Electrophysiological analysis. Recordings were analysed with Clampfit 10.3 (Molecular Devices, Foster City, CA, USA). Inward currents with rise time (10-90% criterion) slower than 10 ms and amplitude greater than 20 pA were classified as SICs. The frequency of control SICs was measured in 8÷12 minutes period before baclofen pressure pulse applications. Baclofen was pressure applied 2-3 times at 5 minute intervals and SICs frequency in the 3 min post stimulus was averaged. All results are presented as mean ± s.e.m. Statistical analyses were performed with two-tailed paired Student's *t*-test except for SICs amplitude and charge transferred for which it was unpaired. Results were considered statistically significant when *p<0.05, **p<0.01, *** p<0.001.

6. References

1. Mulligan, S.J. and B.A. MacVicar, *Calcium transients in astrocyte endfeet cause cerebrovascular constrictions.* Nature, 2004. **431**(7005): p. 195-199.
2. Losi, G., L. Mariotti, and G. Carmignoto, *GABAergic interneuron to astrocyte signalling: a neglected form of cell communication in the brain.* Philosophical Transactions of the Royal Society of London. Series B, Biological Sciences, 2014. **369**(1654).
3. Harris, K.D. and T.D. Mrsic-Flogel, *Cortical connectivity and sensory coding.* Nature, 2013. **503**(7474): p. 51-8.
4. Haydon, P.G. and G. Carmignoto, *Astrocyte control of synaptic transmission and neurovascular coupling.* Physiological Reviews, 2006. **86**(3): p. 1009-31.
5. Araque, A., et al., *Gliotransmitters Travel in Time and Space.* Neuron, 2014. **81**(4): p. 728-739.
6. Volterra, A. and J. Meldolesi, *Astrocytes, from brain glue to communication elements: the revolution continues.* Nature Reviews. Neuroscience, 2005. **6**(8): p. 626-40.
7. Seifert, G., K. Schilling, and C. Steinhauser, *Astrocyte dysfunction in neurological disorders: a molecular perspective.* Nature Reviews. Neuroscience, 2006. **7**(3): p. 194-206.
8. Halassa, M.M., et al., *Synaptic islands defined by the territory of a single astrocyte.* The Journal of Neuroscience, 2007. **27**(24): p. 6473-7.
9. Bernardinelli, Y., D. Muller, and I. Nikonenko, *Astrocyte-synapse structural plasticity.* Neural Plasticity, 2014. **2014**: p. 232105.
10. Perea, G., M. Navarrete, and A. Araque, *Tripartite synapses: astrocytes process and control synaptic information.* Trends in Neurosciences, 2009. **32**(8): p. 421-31.
11. Hirrlinger, J., S. Hulsmann, and F. Kirchhoff, *Astroglial processes show spontaneous motility at active synaptic terminals in situ.* European Journal of Neuroscience, 2004. **20**(8): p. 2235-9.

12. Nestor, M.W., et al., *Plasticity of neuron-glial interactions mediated by astrocytic EphARs.* The Journal of Neuroscience, 2007. **27**(47): p. 12817-28.
13. Nishida, H. and S. Okabe, *Direct astrocytic contacts regulate local maturation of dendritic spines.* The Journal of Neuroscience, 2007. **27**(2): p. 331-40.
14. Perez-Alvarez, A., et al., *Structural and functional plasticity of astrocyte processes and dendritic spine interactions.* The Journal of Neuroscience, 2014. **34**(38): p. 12738-44.
15. Magistretti, P.J., et al., *Energy on demand.* Science, 1999. **283**(5401): p. 496-7.
16. Tsacopoulos, M., *Metabolic signaling between neurons and glial cells: a short review.* Journal of Physiology, Paris, 2002. **96**(3-4): p. 283-8.
17. Peters, A., S.L. Palay, and H.d.F. Webster, in *The fine structure of the central nervous system: Neurons and their supportive cells.*, O.U. Press, Editor. 1991, Oxford University Press: New York. p. 276-295.
18. Halassa, M.M., et al., *Integrated brain circuits: neuron-astrocyte interaction in sleep-related rhythmogenesis.* TheScientificWorldJournal, 2010. **10**: p. 1634-45.
19. Verkhratsky, A., R.K. Orkand, and H. Kettenmann, *Glial calcium: homeostasis and signaling function.* Physiological Reviews, 1998. **78**(1): p. 99-141.
20. Fresu, L., et al., *Plasma membrane calcium ATPase isoforms in astrocytes.* Glia, 1999. **28**(2): p. 150-5.
21. Allaman, I., M. Belanger, and P.J. Magistretti, *Astrocyte-neuron metabolic relationships: for better and for worse.* Trends in Neurosciences, 2011. **34**(2): p. 76-87.
22. Perea, G. and A. Araque, *Properties of synaptically evoked astrocyte calcium signal reveal synaptic information processing by astrocytes.* The Journal of Neuroscience, 2005. **25**(9): p. 2192-2203.
23. Perea, G. and A. Araque, *Synaptic regulation of the astrocyte calcium signal.* Journal of Neural Transmission, 2005. **112**(1): p. 127-35.

24. Pasti, L., et al., *Intracellular calcium oscillations in astrocytes: a highly plastic, bidirectional form of communication between neurons and astrocytes in situ.* The Journal of Neuroscience, 1997. **17**(20): p. 7817-30.
25. Matyash, V., et al., *Nitric oxide signals parallel fiber activity to Bergmann glial cells in the mouse cerebellar slice.* Molecular and Cellular Neurosciences, 2001. **18**(6): p. 664-670.
26. Di Castro, M.A., et al., *Local Ca^{2+} detection and modulation of synaptic release by astrocytes.* Nature Neuroscience, 2011.
27. Panatier, A., et al., *Astrocytes are endogenous regulators of basal transmission at central synapses.* Cell, 2011. **146**(5): p. 785-98.
28. Bezzi, P., et al., *Astrocytes contain a vesicular compartment that is competent for regulated exocytosis of glutamate.* Nature Neuroscience, 2004. **7**(6): p. 613-620.
29. Malarkey, E.B. and V. Parpura, *Temporal characteristics of vesicular fusion in astrocytes: examination of synaptobrevin 2-laden vesicles at single vesicle resolution.* The Journal of Physiology, 2011. **589**(Pt 17): p. 4271-300.
30. Fellin, T., et al., *Neuronal synchrony mediated by astrocytic glutamate through activation of extrasynaptic NMDA receptors.* Neuron, 2004. **43**(5): p. 729-743.
31. Jourdain, P., et al., *Glutamate exocytosis from astrocytes controls synaptic strength.* Nature Neuroscience, 2007. **10**(3): p. 331-9.
32. Perea, G. and A. Araque, *Astrocytes potentiate transmitter release at single hippocampal synapses.* Science, 2007. **317**(5841): p. 1083-6.
33. Pascual, O., et al., *Astrocytic purinergic signaling coordinates synaptic networks.* Science, 2005. **310**(5745): p. 113-6.
34. Serrano, A., et al., *GABAergic network activation of glial cells underlies hippocampal heterosynaptic depression.* The Journal of Neuroscience, 2006. **26**(20): p. 5370-82.
35. Navarrete, M. and A. Araque, *Endocannabinoids mediate neuron-astrocyte communication.* Neuron, 2008. **57**(6): p. 883-93.

36. Navarrete, M. and A. Araque, *Endocannabinoids potentiate synaptic transmission through stimulation of astrocytes.* Neuron, 2010. **68**(1): p. 113-26.
37. Min, R. and T. Nevian, *Astrocyte signaling controls spike timing-dependent depression at neocortical synapses.* Nature Neuroscience, 2012.
38. Henneberger, C., et al., *Long-term potentiation depends on release of D-serine from astrocytes.* Nature, 2010. **463**(7278): p. 232-6.
39. Takata, N., et al., *Astrocyte calcium signaling transforms cholinergic modulation to cortical plasticity in vivo.* The Journal of Neuroscience, 2011. **31**(49): p. 18155-65.
40. Angulo, M.C., et al., *Glutamate released from glial cells synchronizes neuronal activity in the hippocampus.* The Journal of Neuroscience, 2004. **24**(31): p. 6920-6927.
41. Araque, A., et al., *Glutamate-dependent astrocyte modulation of synaptic transmission between cultured hippocampal neurons.* European Journal of Neuroscience, 1998. **10**(6): p. 2129-42.
42. Isaacson, J.S. and M. Scanziani, *How inhibition shapes cortical activity.* Neuron, 2011. **72**(2): p. 231-43.
43. Freund, T.F. and G. Buzsaki, *Interneurons of the hippocampus.* Hippocampus, 1996. **6**(4): p. 347-470.
44. Kawaguchi, Y. and Y. Kubota, *GABAergic cell subtypes and their synaptic connections in rat frontal cortex.* Cerebral Cortex, 1997. **7**(6): p. 476-86.
45. Markram, H., et al., *Interneurons of the neocortical inhibitory system.* Nature Reviews. Neuroscience, 2004. **5**(10): p. 793-807.
46. Ascoli, G.A., et al., *Petilla terminology: nomenclature of features of GABAergic interneurons of the cerebral cortex.* Nature Reviews. Neuroscience, 2008. **9**(7): p. 557-68.
47. Gao, W.J., Y. Wang, and P.S. Goldman-Rakic, *Dopamine modulation of perisomatic and peridendritic inhibition in prefrontal cortex.* The Journal of Neuroscience, 2003. **23**(5): p. 1622-30.

48. Bacci, A., J.R. Huguenard, and D.A. Prince, *Modulation of neocortical interneurons: extrinsic influences and exercises in self-control.* Trends in Neurosciences, 2005. **28**(11): p. 602-10.
49. Fanselow, E.E. and B.W. Connors, *The roles of somatostatin-expressing (GIN) and fast-spiking inhibitory interneurons in UP-DOWN states of mouse neocortex.* Journal of Neurophysiology, 2010. **104**(2): p. 596-606.
50. Kruglikov, I. and B. Rudy, *Perisomatic GABA release and thalamocortical integration onto neocortical excitatory cells are regulated by neuromodulators.* Neuron, 2008. **58**(6): p. 911-24.
51. Rudy, B., et al., *Three groups of interneurons account for nearly 100% of neocortical GABAergic neurons.* Developmental Neurobiology, 2011. **71**(1): p. 45-61.
52. Pouille, F. and M. Scanziani, *Enforcement of temporal fidelity in pyramidal cells by somatic feed-forward inhibition.* Science, 2001. **293**(5532): p. 1159-63.
53. Klausberger, T. and P. Somogyi, *Neuronal diversity and temporal dynamics: the unity of hippocampal circuit operations.* Science, 2008. **321**(5885): p. 53-7.
54. Haider, B. and D.A. McCormick, *Rapid neocortical dynamics: cellular and network mechanisms.* Neuron, 2009. **62**(2): p. 171-89.
55. Pfeffer, C.K., et al., *Inhibition of inhibition in visual cortex: the logic of connections between molecularly distinct interneurons.* Nature Neuroscience, 2013. **16**(8): p. 1068-76.
56. Xu, H., et al., *Neocortical somatostatin-expressing GABAergic interneurons disinhibit the thalamorecipient layer 4.* Neuron, 2013. **77**(1): p. 155-67.
57. Lewis, D.A. and G. Gonzalez-Burgos, *Pathophysiologically based treatment interventions in schizophrenia.* Nature Medicine, 2006. **12**(9): p. 1016-22.
58. Thomson, A.M. and C. Lamy, *Functional maps of neocortical local circuitry.* Frontiers in Neuroscience, 2007. **1**(1): p. 19-42.

59. Silberberg, G. and H. Markram, *Disynaptic inhibition between neocortical pyramidal cells mediated by Martinotti cells.* Neuron, 2007. **53**(5): p. 735-46.
60. Wang, Y., et al., *Anatomical, physiological and molecular properties of Martinotti cells in the somatosensory cortex of the juvenile rat.* The Journal of Physiology, 2004. **561**(Pt 1): p. 65-90.
61. Adesnik, H., et al., *A neural circuit for spatial summation in visual cortex.* Nature, 2012. **490**(7419): p. 226-31.
62. Gentet, L.J., et al., *Unique functional properties of somatostatin-expressing GABAergic neurons in mouse barrel cortex.* Nature Neuroscience, 2012. **15**(4): p. 607-12.
63. Cauli, B., et al., *Molecular and physiological diversity of cortical nonpyramidal cells.* The Journal of Neuroscience, 1997. **17**(10): p. 3894-906.
64. Porter, J.T., et al., *Properties of bipolar VIPergic interneurons and their excitation by pyramidal neurons in the rat neocortex.* European Journal of Neuroscience, 1998. **10**(12): p. 3617-28.
65. Ferezou, I., et al., *5-HT_3 receptors mediate serotonergic fast synaptic excitation of neocortical vasoactive intestinal peptide/cholecystokinin interneurons.* The Journal of Neuroscience, 2002. **22**(17): p. 7389-97.
66. Galarreta, M., et al., *Electrical coupling among irregular-spiking GABAergic interneurons expressing cannabinoid receptors.* The Journal of Neuroscience, 2004. **24**(44): p. 9770-8.
67. Miyoshi, G., et al., *Genetic fate mapping reveals that the caudal ganglionic eminence produces a large and diverse population of superficial cortical interneurons.* The Journal of Neuroscience, 2010. **30**(5): p. 1582-94.
68. Butt, S.J., et al., *The temporal and spatial origins of cortical interneurons predict their physiological subtype.* Neuron, 2005. **48**(4): p. 591-604.
69. Runquist, M. and G. Alonso, *Gabaergic signaling mediates the morphological organization of astrocytes in the adult rat forebrain.* Glia, 2003. **41**(2): p. 137-51.

70. Lee, M., C. Schwab, and P.L. McGeer, *Astrocytes are GABAergic cells that modulate microglial activity.* Glia, 2011. **59**(1): p. 152-65.
71. Kettenmann, H., K.H. Backus, and M. Schachner, *Aspartate, glutamate and gamma-aminobutyric acid depolarize cultured astrocytes.* Neuroscience Letters, 1984. **52**(1-2): p. 25-9.
72. Kettenmann, H. and M. Schachner, *Pharmacological properties of γ-aminobutyric acid-, glutamate-, and aspartate-induced depolarizations in cultured astrocytes.* The Journal of Neuroscience, 1985. **5**(12): p. 3295-301.
73. Backus, K.H., H. Kettenmann, and M. Schachner, *Effect of benzodiazepines and pentobarbital on the GABA-induced depolarization in cultured astrocytes.* Glia, 1988. **1**(2): p. 132-40.
74. Fraser, D.D., et al., *$GABA_A$/benzodiazepine receptors in acutely isolated hippocampal astrocytes.* The Journal of Neuroscience, 1995. **15**(4): p. 2720-32.
75. MacVicar, B.A., et al., *GABA-activated Cl^- channels in astrocytes of hippocampal slices.* The Journal of Neuroscience, 1989. **9**(10): p. 3577-83.
76. Clark, B. and P. Mobbs, *Transmitter-operated channels in rabbit retinal astrocytes studied in situ by whole-cell patch clamping.* The Journal of Neuroscience, 1992. **12**(2): p. 664-73.
77. Muller, T., et al., *Developmental regulation of voltage-gated K^+ channel and $GABA_A$ receptor expression in Bergmann glial cells.* The Journal of Neuroscience, 1994. **14**(5 Pt 1): p. 2503-14.
78. Steinhauser, C., R. Jabs, and H. Kettenmann, *Properties of GABA and glutamate responses in identified glial cells of the mouse hippocampal slice.* Hippocampus, 1994. **4**(1): p. 19-35.
79. Egawa, K., et al., *Cl^- homeodynamics in gap-junction-coupled astrocytic networks on activation of GABAergic synapses.* The Journal of Physiology, 2013. **591**(Pt 16): p. 3901-17.
80. Rosewater, K. and H. Sontheimer, *Fibrous and protoplasmic astrocytes express $GABA_A$ receptors that differ in benzodiazepine pharmacology.* Brain Research, 1994. **636**(1): p. 73-80.

81. Kang, J., et al., *Astrocyte-mediated potentiation of inhibitory synaptic transmission.* Nature Neuroscience, 1998. **1**(8): p. 683-692.
82. Nilsson, M., et al., *GABA induces Ca^{2+} transients in astrocytes.* Neuroscience, 1993. **54**(3): p. 605-14.
83. Meier, S.D., K.W. Kafitz, and C.R. Rose, *Developmental profile and mechanisms of GABA-induced calcium signaling in hippocampal astrocytes.* Glia, 2008. **56**(10): p. 1127-37.
84. Bettler, B., et al., *Molecular structure and physiological functions of $GABA_B$ receptors.* Physiological Reviews, 2004. **84**(3): p. 835-67.
85. Doengi, M., et al., *GABA uptake-dependent Ca^{2+} signaling in developing olfactory bulb astrocytes.* Proceedings of the National Academy of Sciences of the United States of America, 2009. **106**(41): p. 17570-5.
86. Andersson, M., F. Blomstrand, and E. Hanse, *Astrocytes play a critical role in transient heterosynaptic depression in the rat hippocampal CA1 region.* The Journal of Physiology, 2007. **585**(Pt 3): p. 843-52.
87. Nusser, Z. and I. Mody, *Selective modulation of tonic and phasic inhibitions in dentate gyrus granule cells.* Journal of Neurophysiology, 2002. **87**(5): p. 2624-8.
88. Semyanov, A., et al., *Tonically active $GABA_A$ receptors: modulating gain and maintaining the tone.* Trends in Neurosciences, 2004. **27**(5): p. 262-9.
89. Farrant, M. and Z. Nusser, *Variations on an inhibitory theme: phasic and tonic activation of $GABA_A$ receptors.* Nature Reviews. Neuroscience, 2005. **6**(3): p. 215-29.
90. Minelli, A., et al., *GAT-1, a high-affinity GABA plasma membrane transporter, is localized to neurons and astroglia in the cerebral cortex.* The Journal of Neuroscience, 1995. **15**(11): p. 7734-46.
91. Conti, F., et al., *Neuronal and glial localization of GAT-1, a high-affinity □-aminobutyric acid plasma membrane transporter, in human cerebral cortex: with a note on its distribution in monkey cortex.* The Journal of Comparative Neurology, 1998. **396**(1): p. 51-63.

92. Melone, M., S. Ciappelloni, and F. Conti, *A quantitative analysis of cellular and synaptic localization of GAT-1 and GAT-3 in rat neocortex.* Brain Structure & Function, 2013.
93. Kersanté, F., et al., *A functional role for both γ-aminobutyric acid (GABA) transporter-1 and GABA transporter-3 in the modulation of extracellular GABA and GABAergic tonic conductances in the rat hippocampus.* The Journal of Physiology, 2013. **591**(Pt 10): p. 2429-41.
94. Beenhakker, M.P. and J.R. Huguenard, *Astrocytes as gatekeepers of $GABA_B$ receptor function.* The Journal of Neuroscience, 2010. **30**(45): p. 15262-76.
95. De Biasi, S., L. Vitellaro-Zuccarello, and N.C. Brecha, *Immunoreactivity for the GABA transporter-1 and GABA transporter-3 is restricted to astrocytes in the rat thalamus. A light and electron-microscopic immunolocalization.* Neuroscience, 1998. **83**(3): p. 815-28.
96. Vitellaro-Zuccarello, L., N. Calvaresi, and S. De Biasi, *Expression of GABA transporters, GAT-1 and GAT-3, in the cerebral cortex and thalamus of the rat during postnatal development.* Cell and Tissue Research, 2003. **313**(3): p. 245-57.
97. Cope, D.W., et al., *Enhanced tonic $GABA_A$ inhibition in typical absence epilepsy.* Nature Medicine, 2009. **15**(12): p. 1392-8.
98. Pirttimaki, T., H.R. Parri, and V. Crunelli, *Astrocytic GABA transporter GAT-1 dysfunction in experimental absence seizures.* The Journal of Physiology, 2013. **591**(Pt 4): p. 823-33.
99. Shigetomi, E., et al., *TRPA1 channels regulate astrocyte resting calcium and inhibitory synapse efficacy through GAT-3.* Nature Neuroscience, 2012. **15**(1): p. 70-80.
100. Heja, L., et al., *Glutamate uptake triggers transporter-mediated GABA release from astrocytes.* PloS One, 2009. **4**(9): p. e7153.
101. Heja, L., et al., *Astrocytes convert network excitation to tonic inhibition of neurons.* BMC Biology, 2012. **10**: p. 26.
102. Martin, D.L. and K. Rimvall, *Regulation of gamma-aminobutyric acid synthesis in the brain.* Journal of Neurochemistry, 1993. **60**(2): p. 395-407.

103. Ochi, S., et al., *Transient presence of GABA in astrocytes of the developing optic nerve.* Glia, 1993. **9**(3): p. 188-98.
104. Yoon, B.E., J. Woo, and C.J. Lee, *Astrocytes as GABA-ergic and GABA-ceptive cells.* Neurochemical Research, 2012. **37**(11): p. 2474-9.
105. Seiler, N., M.J. al-Therib, and K. Kataoka, *Formation of GABA from putrescine in the brain of fish (Salmo irideus Gibb.).* Journal of Neurochemistry, 1973. **20**(3): p. 699-708.
106. Seiler, N. and A. Askar, *A micro method for the quantitative estimation of putrescine in tissues.* Journal of Chromatography, 1971. **62**(1): p. 121-7.
107. Kremzner, L.T., J.M. Hiller, and E.J. Simon, *Metabolism of polyamines in mouse neuroblastoma cells in culture: formation of GABA and putreanine.* Journal of Neurochemistry, 1975. **25**(6): p. 889-94.
108. Kozlov, A.S., et al., *Target cell-specific modulation of neuronal activity by astrocytes.* Proceedings of the National Academy of Sciences of the United States of America, 2006. **103**(26): p. 10058-63.
109. Jimenez-Gonzalez, C., et al., *Non-neuronal, slow GABA signalling in the ventrobasal thalamus targets □-subunit-containing $GABA_A$ receptors.* European Journal of Neuroscience, 2011. **33**(8): p. 1471-82.
110. Le Meur, K., et al., *GABA release by hippocampal astrocytes.* Frontiers in Computational Neuroscience, 2012. **6**: p. 59.
111. Parri, H.R., T.M. Gould, and V. Crunelli, *Spontaneous astrocytic Ca^{2+} oscillations in situ drive NMDAR-mediated neuronal excitation.* Nature Neuroscience, 2001. **4**(8): p. 803-12.
112. D'Ascenzo, M., et al., *mGluR5 stimulates gliotransmission in the nucleus accumbens.* Proceedings of the National Academy of Sciences of the United States of America, 2007. **104**(6): p. 1995-2000.
113. Shigetomi, E., et al., *Two forms of astrocyte calcium excitabilty have distinct effects on NMDA receptor-mediated slow inward currents in pyramidal neurons.* The Journal of Neuroscience, 2008. **28**: p. 6659-6663.
114. Pirttimaki, T.M., et al., *□7 Nicotinic receptor-mediated astrocytic gliotransmitter release: A □ effects in a p model.* PloS One, 2013. **8**(11): p. e81828.

115. Lee, S., et al., *Channel-mediated tonic GABA release from glia.* Science, 2010. **330**(6005): p. 790-6.
116. Yoon, B.E., et al., *The amount of astrocytic GABA positively correlates with the degree of tonic inhibition in hippocampal CA1 and cerebellum.* Molecular Brain, 2011. **4**: p. 42.
117. Oh, S.J., et al., *Protease activated receptor 1-induced glutamate release in cultured astrocytes is mediated by Bestrophin-1 channel but not by vesicular exocytosis.* Molecular Brain, 2012. **5**: p. 38.
118. Park, H., et al., *High glutamate permeability and distal localization of Best1 channel in CA1 hippocampal astrocyte.* Molecular Brain, 2013. **6**: p. 54.
119. Lee, M., E.G. McGeer, and P.L. McGeer, *Mechanisms of GABA release from human astrocytes.* Glia, 2011. **59**(11): p. 1600-11.
120. Lalo, U., et al., *Exocytosis of ATP from astrocytes modulates phasic and tonic inhibition in the neocortex.* PLoS Biology, 2014. **12**(1): p. e1001747.
121. Huang, Y.H., et al., *Astrocyte glutamate transporters regulate metabotropic glutamate receptor-mediated excitation of hippocampal interneurons.* The Journal of Neuroscience, 2004. **24**(19): p. 4551-9.
122. Liu, Q.-S., et al., *Astrocyte-mediated activation of neuronal kainate receptors.* Proceedings of the National Academy of Sciences of the United States of America, 2004. **101**(9): p. 3172-3177.
123. Bowser, D.N. and B.S. Khakh, *ATP excites interneurons and astrocytes to increase synaptic inhibition in neuronal networks.* The Journal of Neuroscience, 2004. **24**(39): p. 8606-8620.
124. Rossi, D. and A. Volterra, *Astrocytic dysfunction: insights on the role in neurodegeneration.* Brain Research Bulletin, 2009. **80**(4-5): p. 224-32.
125. Losi, G., M. Cammarota, and G. Carmignoto, *The role of astroglia in the epileptic brain.* Frontiers in Pharmacology, 2012. **3**: p. 132.
126. Puia, G., et al., *Neurosteroids act on recombinant human $GABA_A$ receptors.* Neuron, 1990. **4**(5): p. 759-65.
127. Lambert, J.J., et al., *Neurosteroid modulation of $GABA_A$ receptors.* Progress in Neurobiology, 2003. **71**(1): p. 67-80.

128. Reddy, D.S., *Neurosteroids: endogenous role in the human brain and therapeutic potentials.* Progress in Brain Research, 2010. **186**: p. 113-37.
129. Biagini, G., et al., *Neurosteroids and epileptogenesis in the pilocarpine model: evidence for a relationship between P450scc induction and length of the latent period.* Epilepsia, 2009. **50 Suppl 1**: p. 53-8.
130. Li, X., et al., *Endothelin-1-induced arrhythmogenic Ca^{2+} signaling is abolished in atrial myocytes of inositol-1,4,5-trisphosphate(IP_3)-receptor type 2-deficient mice.* Circulation Research, 2005. **96**(12): p. 1274-81.
131. Charles, K.J., et al., *$GABA_B$ receptor subunit expression in glia.* Molecular and Cellular Neurosciences, 2003. **24**(1): p. 214-23.
132. Charles, K.J., et al., *Distribution of a $GABA_B$-like receptor protein in the rat central nervous system.* Brain Research, 2003. **989**(2): p. 135-46.
133. Velez-Fort, M., E. Audinat, and M.C. Angulo, *Central Role of GABA in Neuron-Glia Interactions.* The Neuroscientist, 2011. **18**(3): p. 237-50.
134. Parpura, V., V. Grubisic, and A. Verkhratsky, *Ca^{2+} sources for the exocytotic release of glutamate from astrocytes.* Biochimica et Biophysica Acta, 2011. **1813**(5): p. 984-91.
135. Verkhratsky, A. and C. Steinhauser, *Ion channels in glial cells.* Brain Research. Brain Research Reviews, 2000. **32**(2-3): p. 380-412.
136. Verkhratsky, A., J.J. Rodriguez, and V. Parpura, *Calcium signalling in astroglia.* Molecular and Cellular Endocrinology, 2012. **353**(1-2): p. 45-56.
137. Guthrie, P.B., et al., *ATP released from astrocytes mediates glial calcium waves.* The Journal of Neuroscience, 1999. **19**(2): p. 520-8.
138. Pierce, K.L., R.T. Premont, and R.J. Lefkowitz, *Seven-transmembrane receptors.* Nature Reviews. Molecular Cell Biology, 2002. **3**(9): p. 639-50.
139. Zeng, W., et al., *A new mode of Ca^{2+} signaling by G protein-coupled receptors: gating of IP_3 receptor Ca^{2+} release channels by G* /Current Biology, 2003. **13**(10): p. 872-6.
140. Theodosis, D.T., D.A. Poulain, and S.H. Oliet, *Activity-dependent structural and functional plasticity of astrocyte-neuron interactions.* Physiological Reviews, 2008. **88**(3): p. 983-1008.

141. Haber, M., L. Zhou, and K.K. Murai, *Cooperative astrocyte and dendritic spine dynamics at hippocampal excitatory synapses.* The Journal of Neuroscience, 2006. **26**(35): p. 8881-91.
142. Freund, T.F. and I. Katona, *Perisomatic inhibition.* Neuron, 2007. **56**(1): p. 33-42.
143. Singer, W., *Neuronal synchrony: a versatile code for the definition of relations?* Neuron, 1999. **24**(1): p. 49-65.
144. Sanchez-Vives, M.V. and D.A. McCormick, *Cellular and network mechanisms of rhythmic recurrent activity in neocortex.* Nat Neurosci, 2000. **3**(10): p. 1027-34.
145. McBain, C.J. and J.A. Kauer, *Presynaptic plasticity: targeted control of inhibitory networks.* Current Opinion in Neurobiology, 2009. **19**(3): p. 254-62.
146. Poskanzer, K.E. and R. Yuste, *Astrocytic regulation of cortical UP states.* Proceedings of the National Academy of Sciences of the United States of America, 2011. **108**(45): p. 18453-8.
147. Farinella, M., et al., *Glutamate-bound NMDARs arising from in vivo-like network activity extend spatio-temporal integration in a L5 cortical pyramidal cell model.* PLoS Computational Biology, 2014. **10**(4): p. e1003590.
148. Cammarota, M., et al., *Fast spiking interneuron control of seizure propagation in a cortical slice model of focal epilepsy.* The Journal of Physiology, 2013. **591**(Pt 4): p. 807-22.
149. Mori, T., et al., *Inducible gene deletion in astroglia and radial glia--a valuable tool for functional and lineage analysis.* Glia, 2006. **54**(1): p. 21-34.